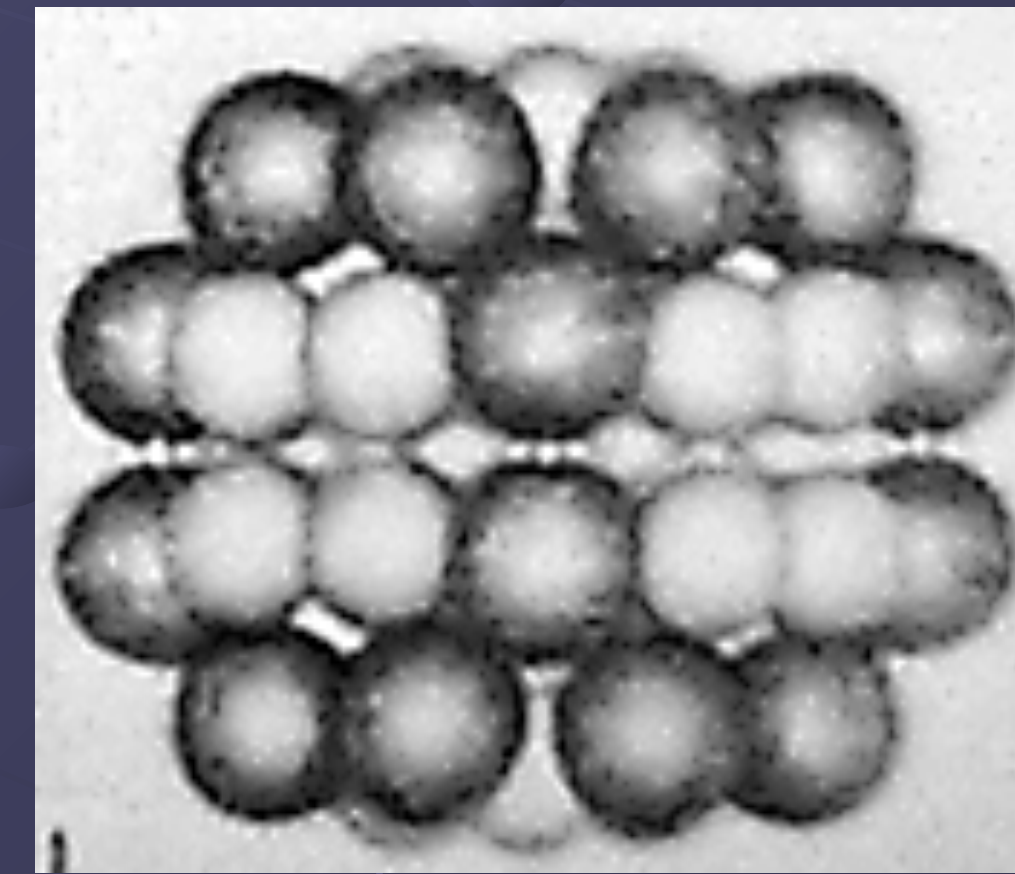
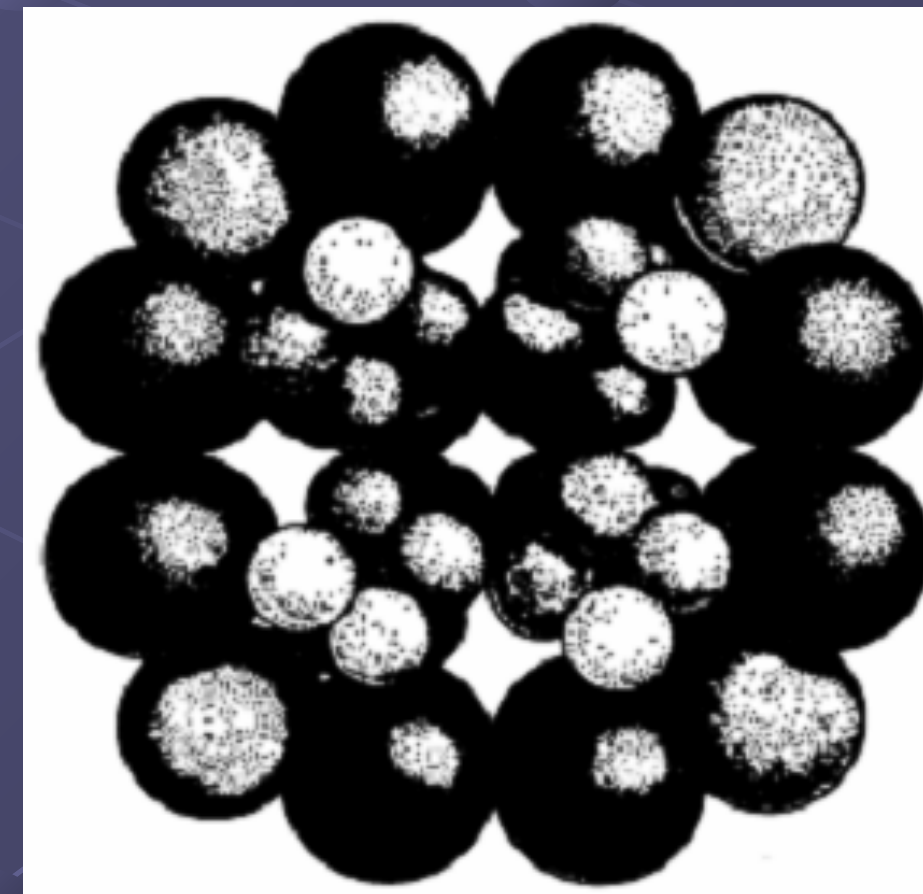
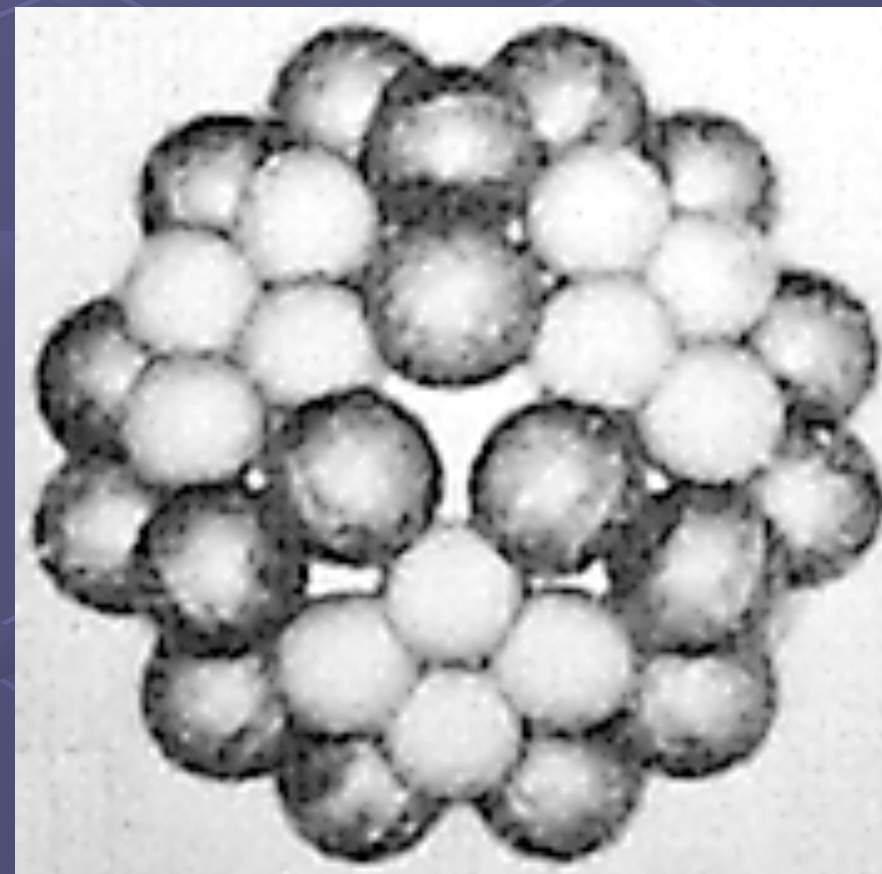
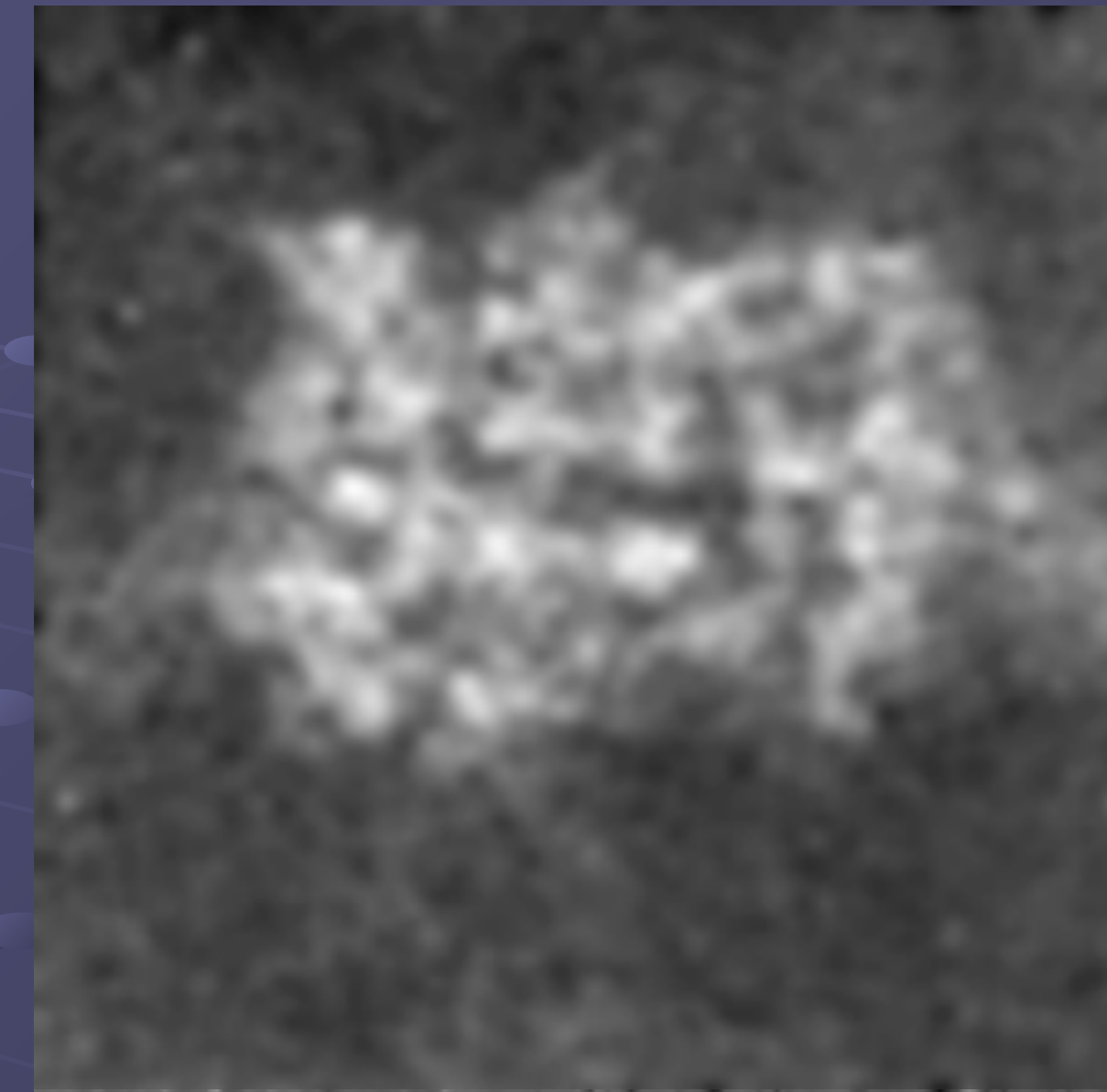
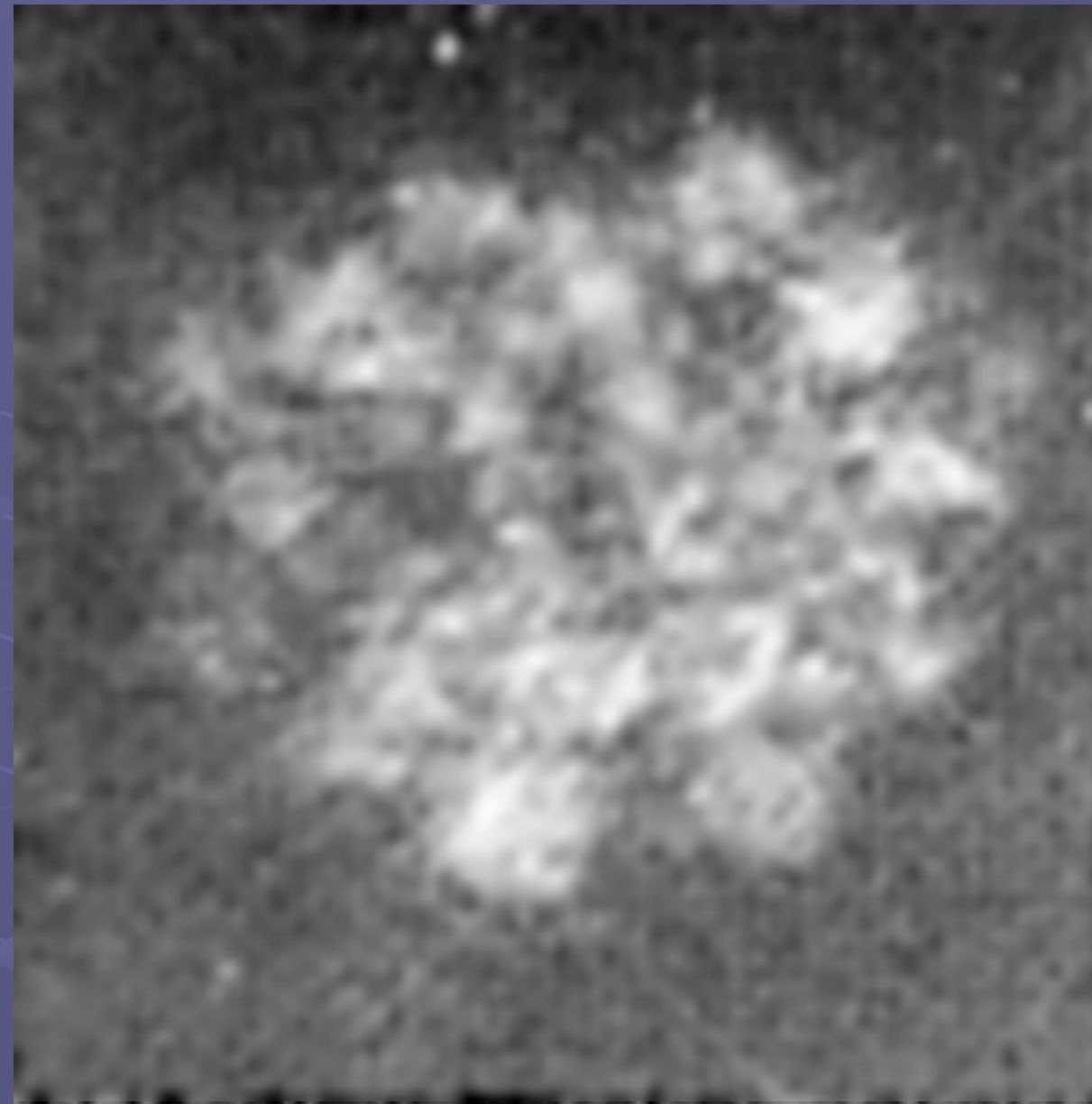


The
**evolution,
deficiencies,
&
promise
of
cryo-electron microscopy**

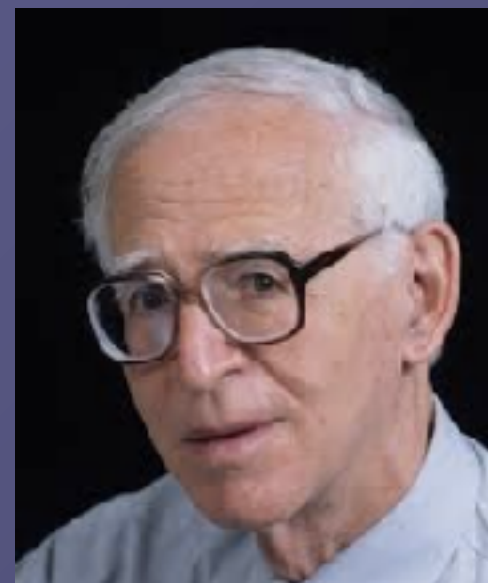
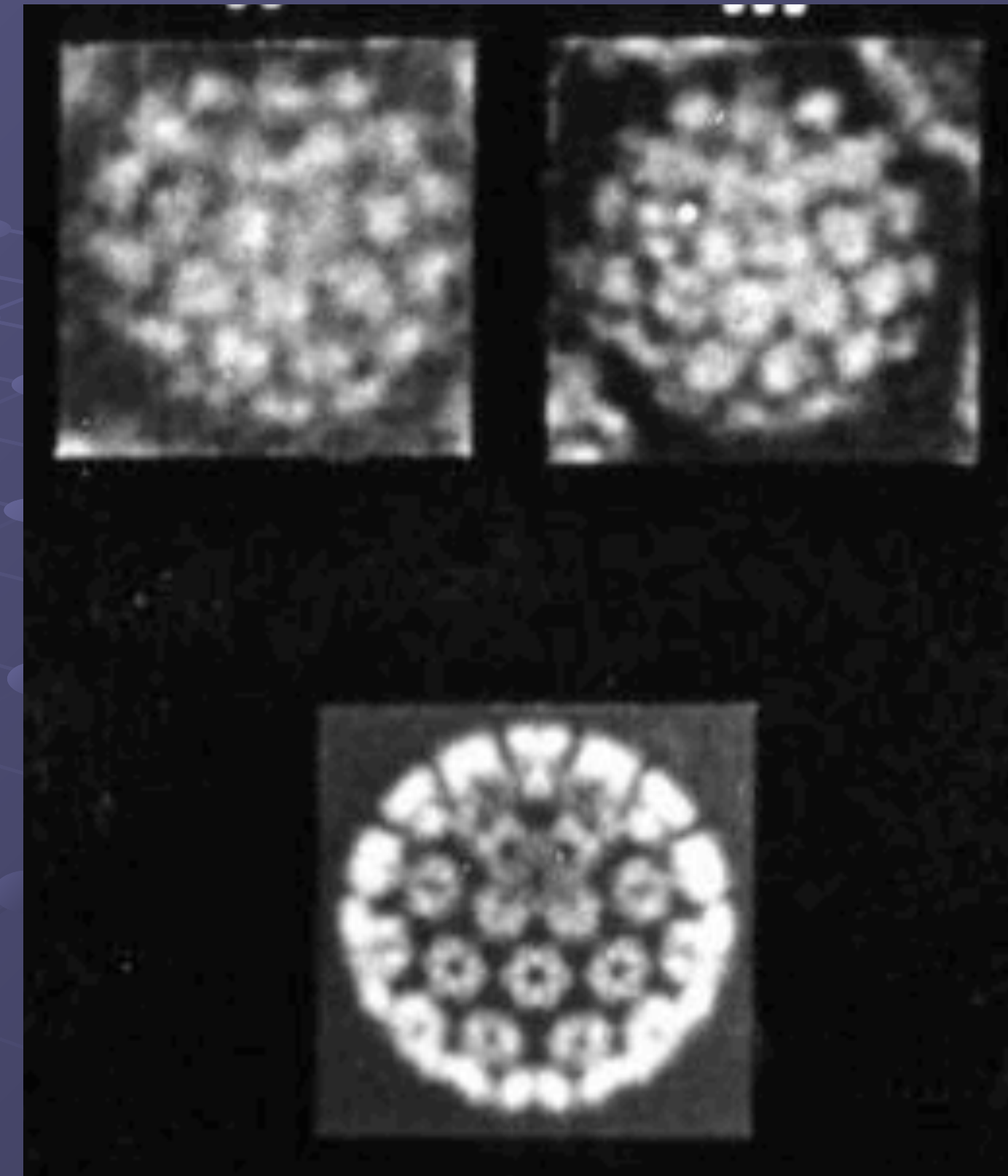
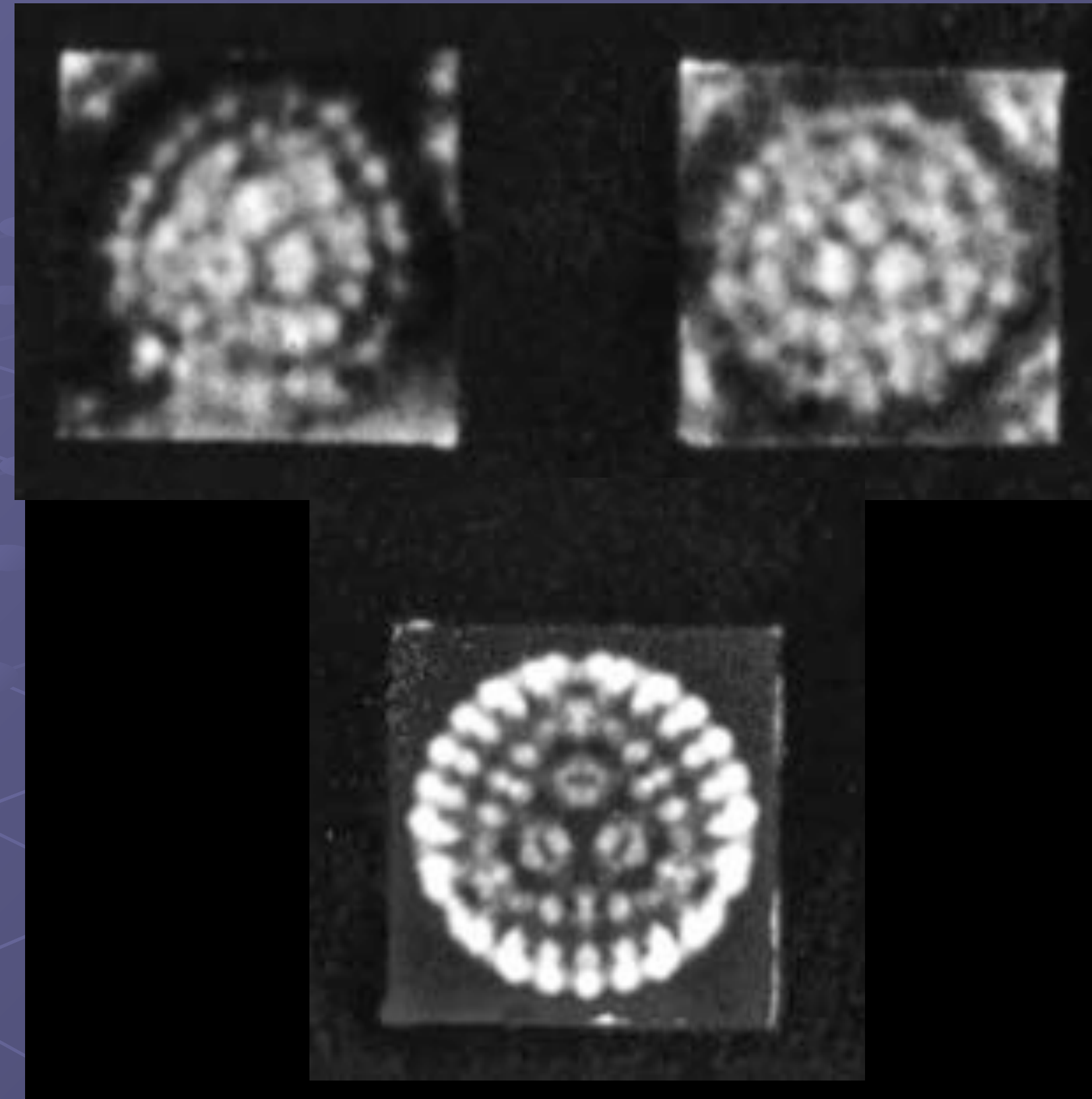
The
evolution,
deficiencies,
&
promise
of
cryo-electron microscopy

Image analysis once consisted of guessing the structure and building a simple model that seemed to account for the images.



(L.J. Reed & D.J. Cox, *The Enzymes*, 1, 213-240, 1970)

Klug and Finch simulated EM images of model structures and compared them in great detail to micrographs of human wart virus.



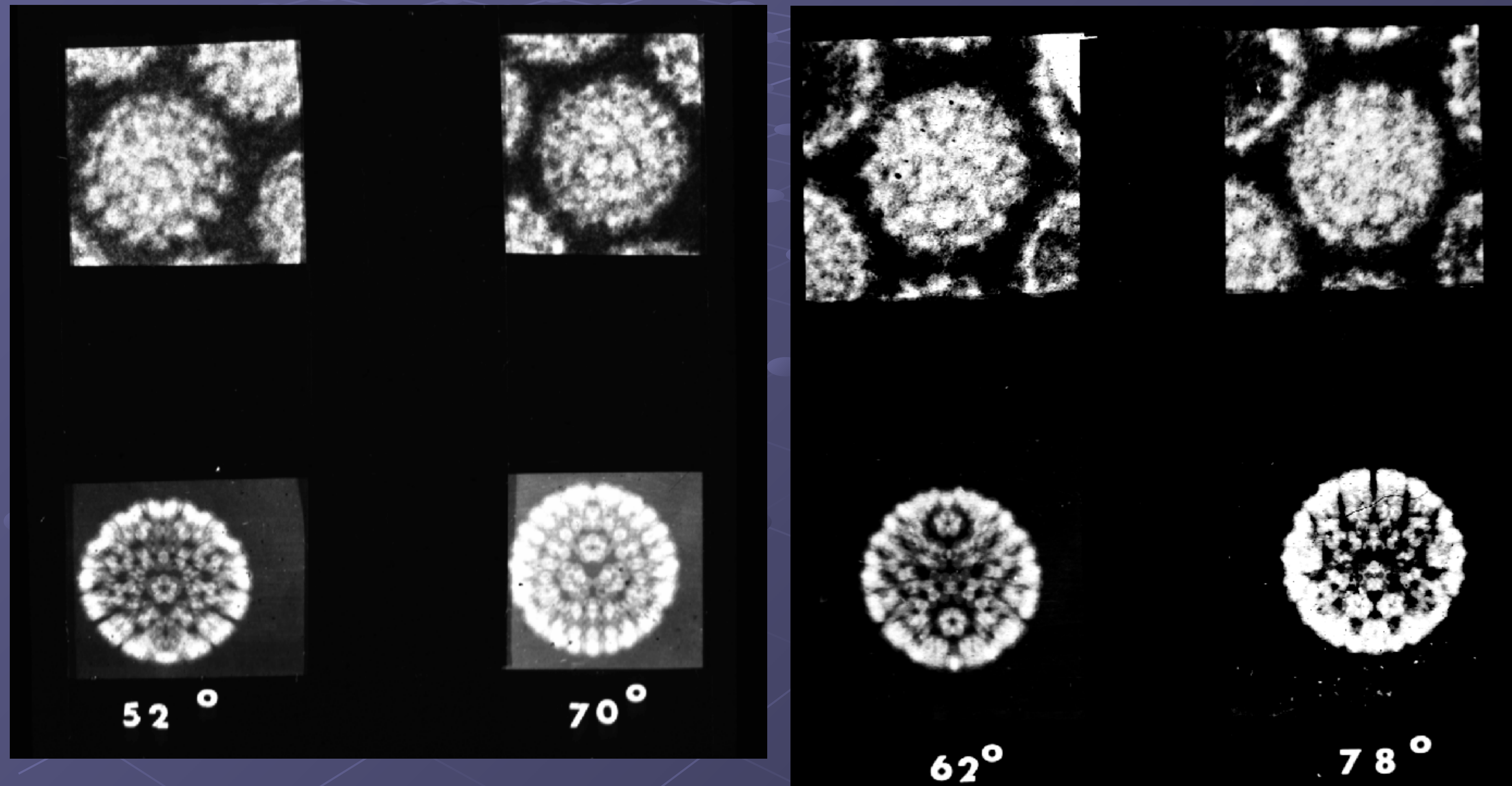
Aaron Klug



John Finch

They tilted the virus in the microscope and the model by the same amount and about the same axis to prove the model was unique.

Here are two $\sim 17^\circ$ tilts:



Structure determination: guess the structure, compare it to images, & tilt.

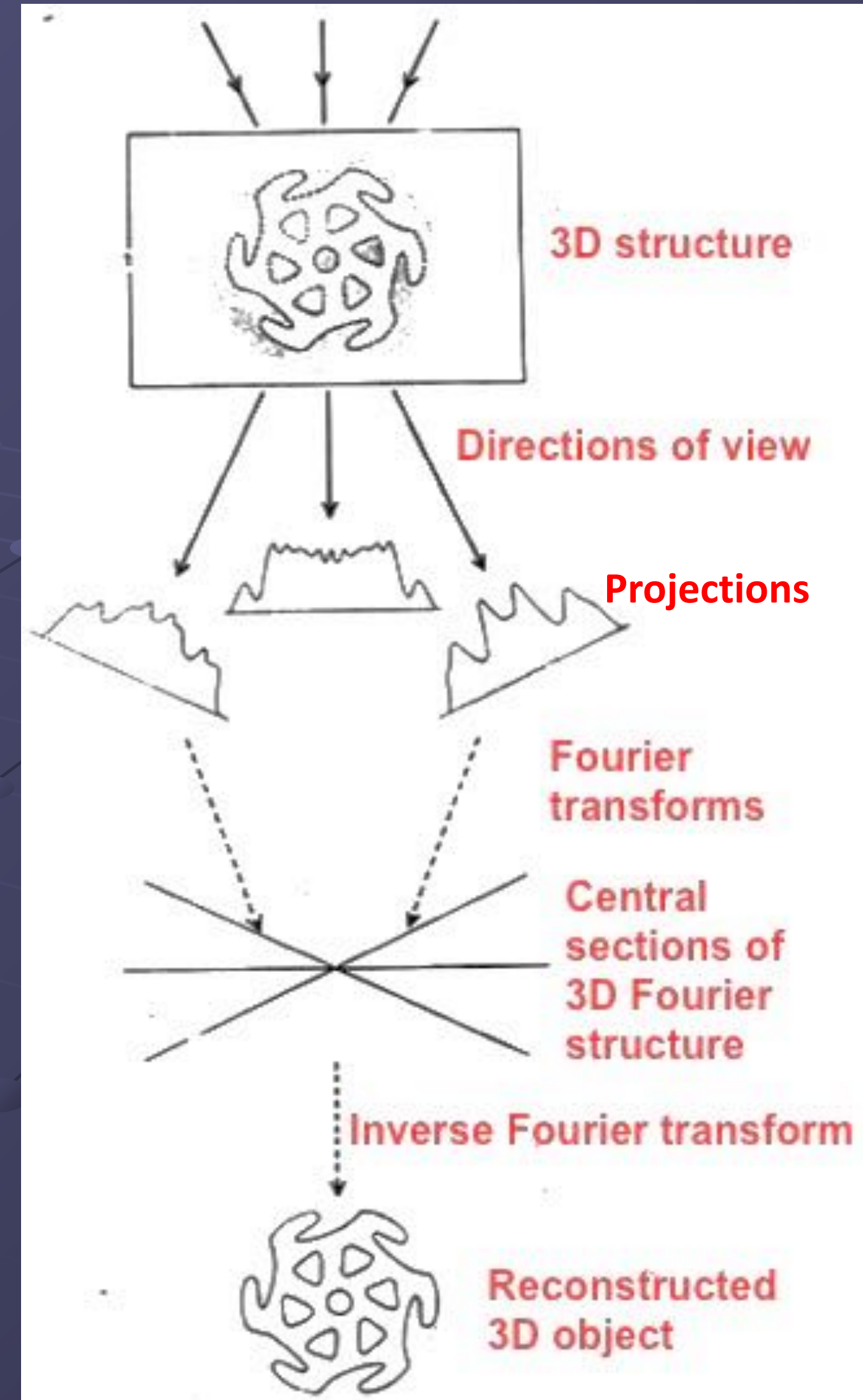
Reconstruction of Three Dimensional Structures from Electron Micrographs

by

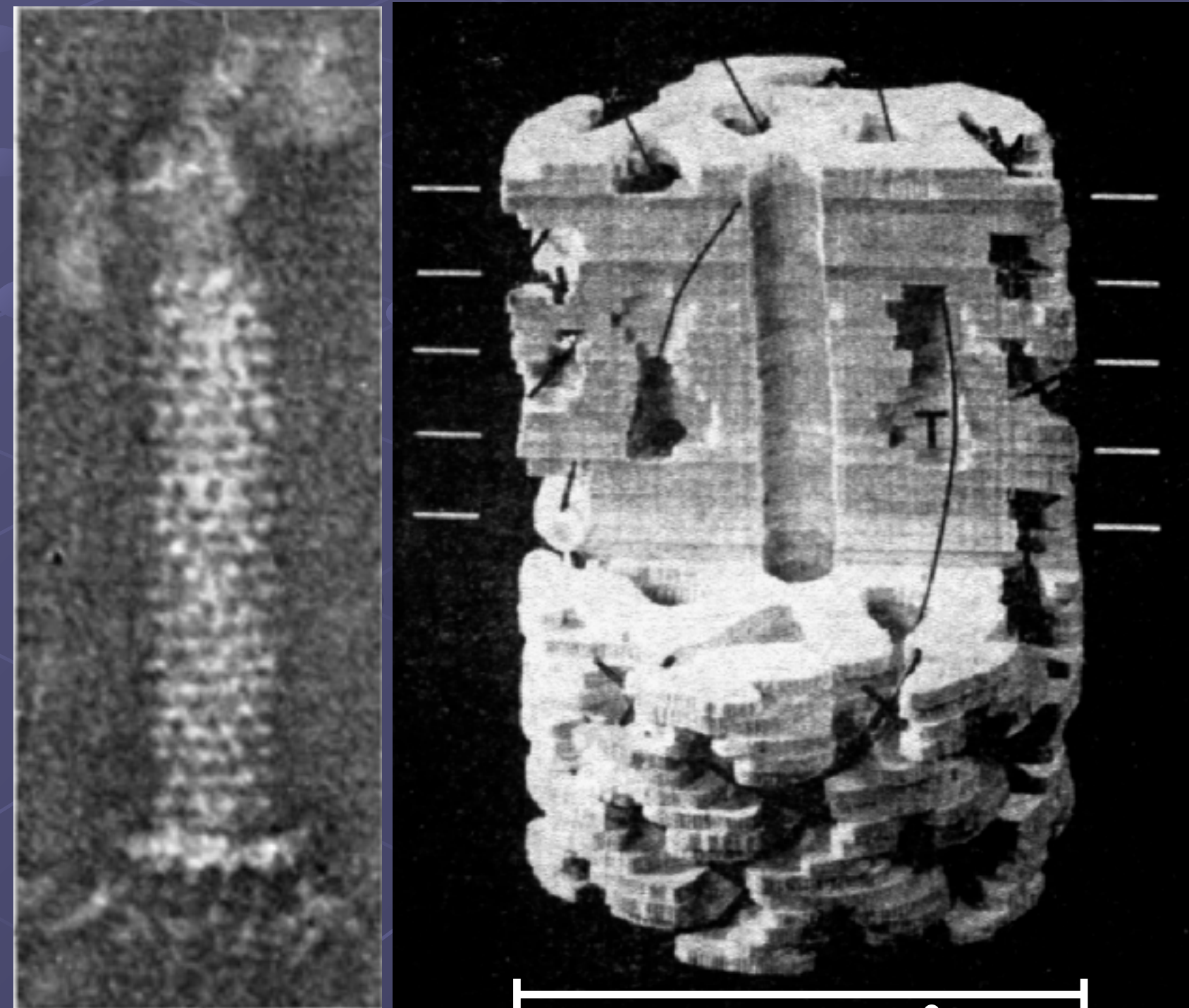
D. J. DE ROSIER
A. KLUG

MRC Laboratory of Molecular Biology,
Hills Road, Cambridge

General principles are formulated for the objective reconstruction of a three dimensional object from a set of electron microscope images. These principles are applied to the calculation of a three dimensional density map of the tail of bacteriophage T4.



Aaron Klug

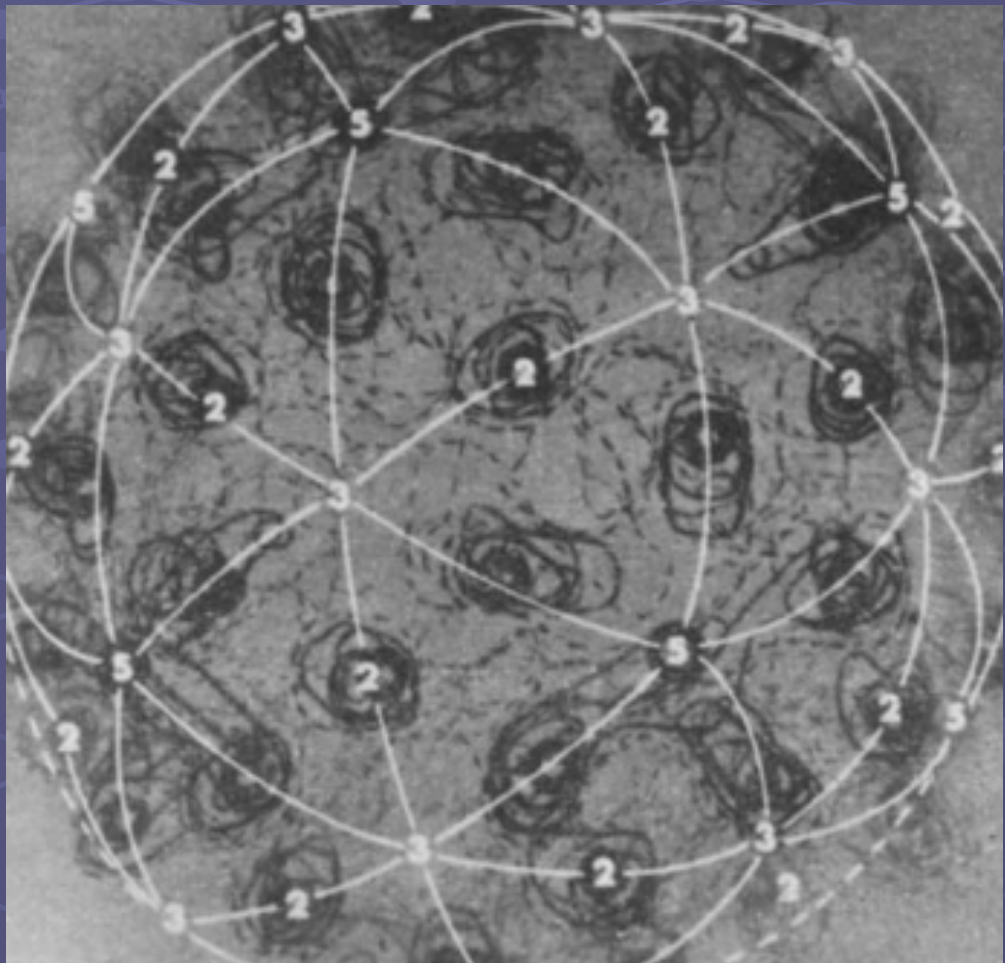


240 Å
resolution = ~35Å

Now there was a general method for solving structures.

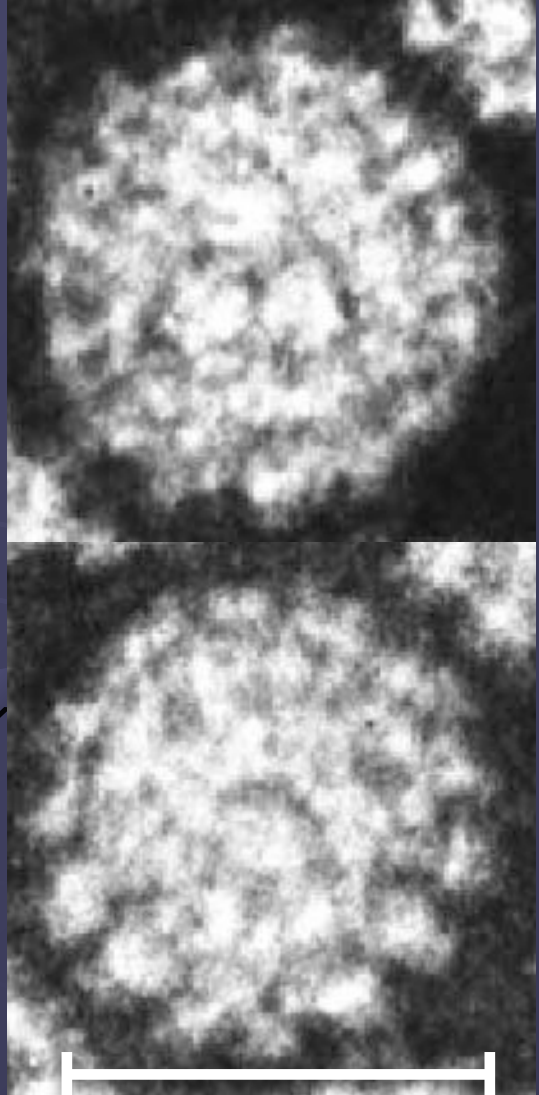
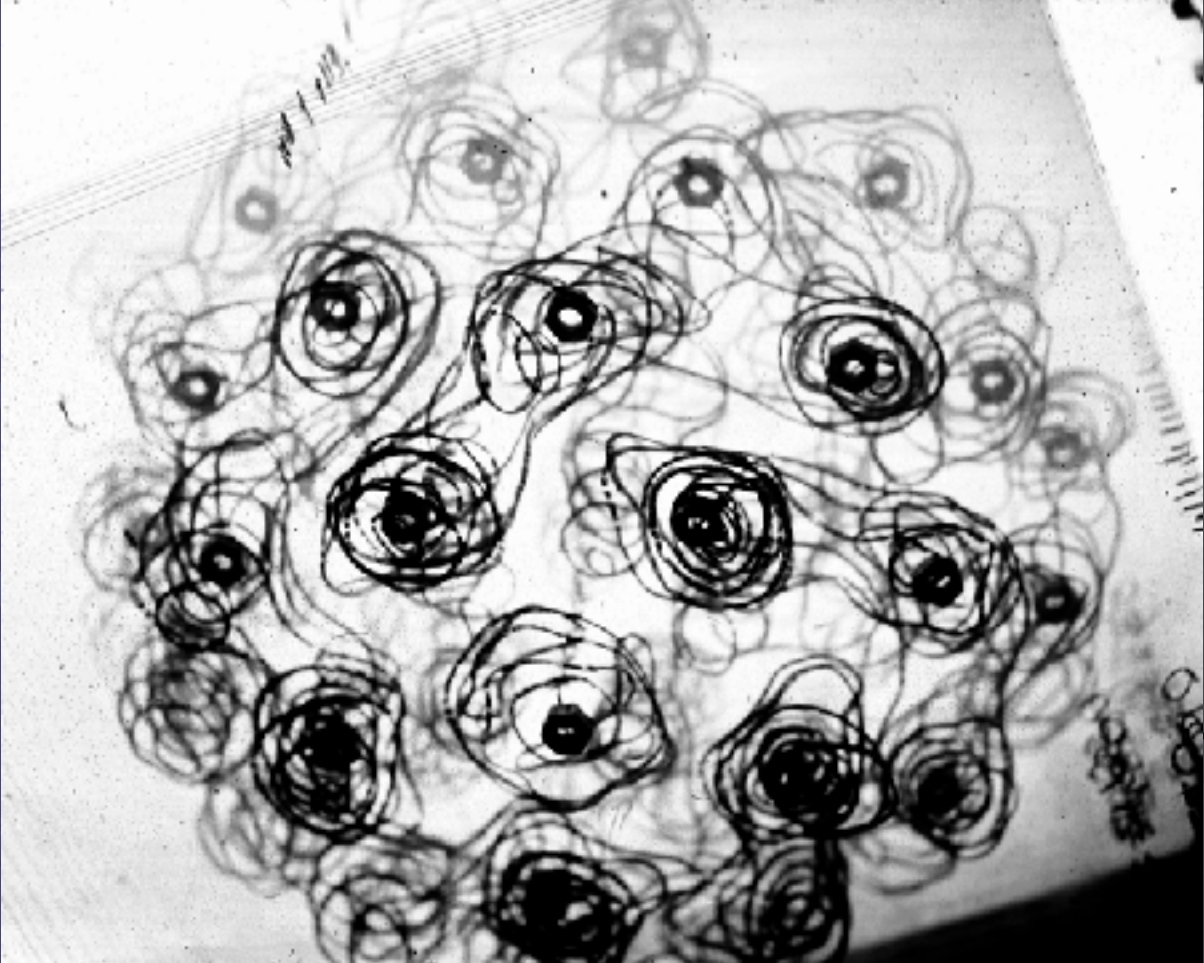
First single particle reconstructions

Tomato bushy stunt virus



resolution = ~28 Å

Human wart virus



resolution = ~60 Å



Tony Crowther

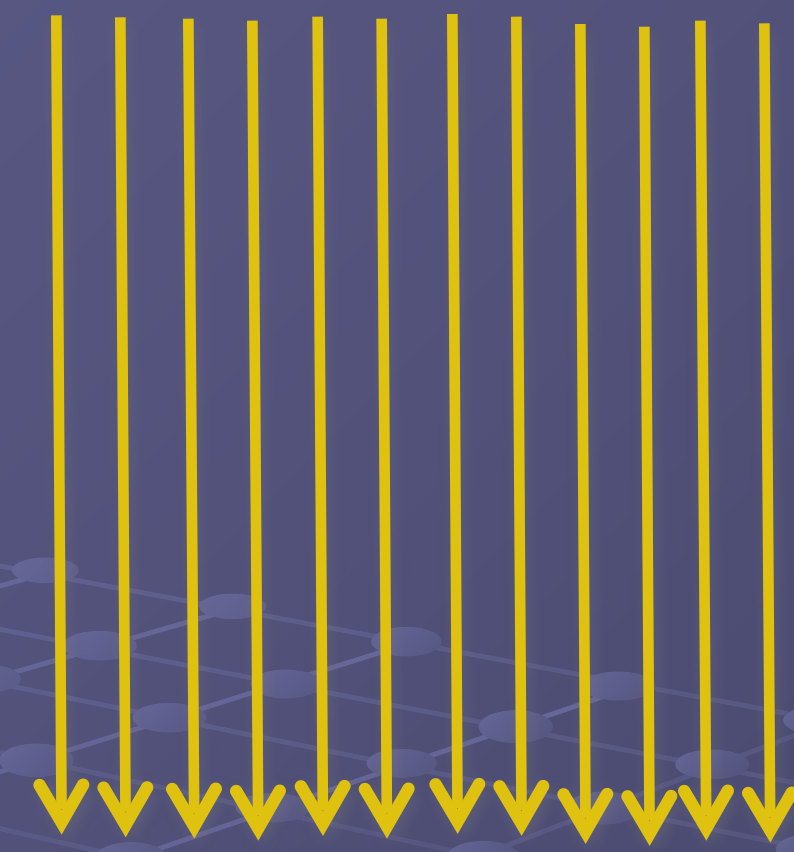


Linda Amos

Molecular resolution by EM!

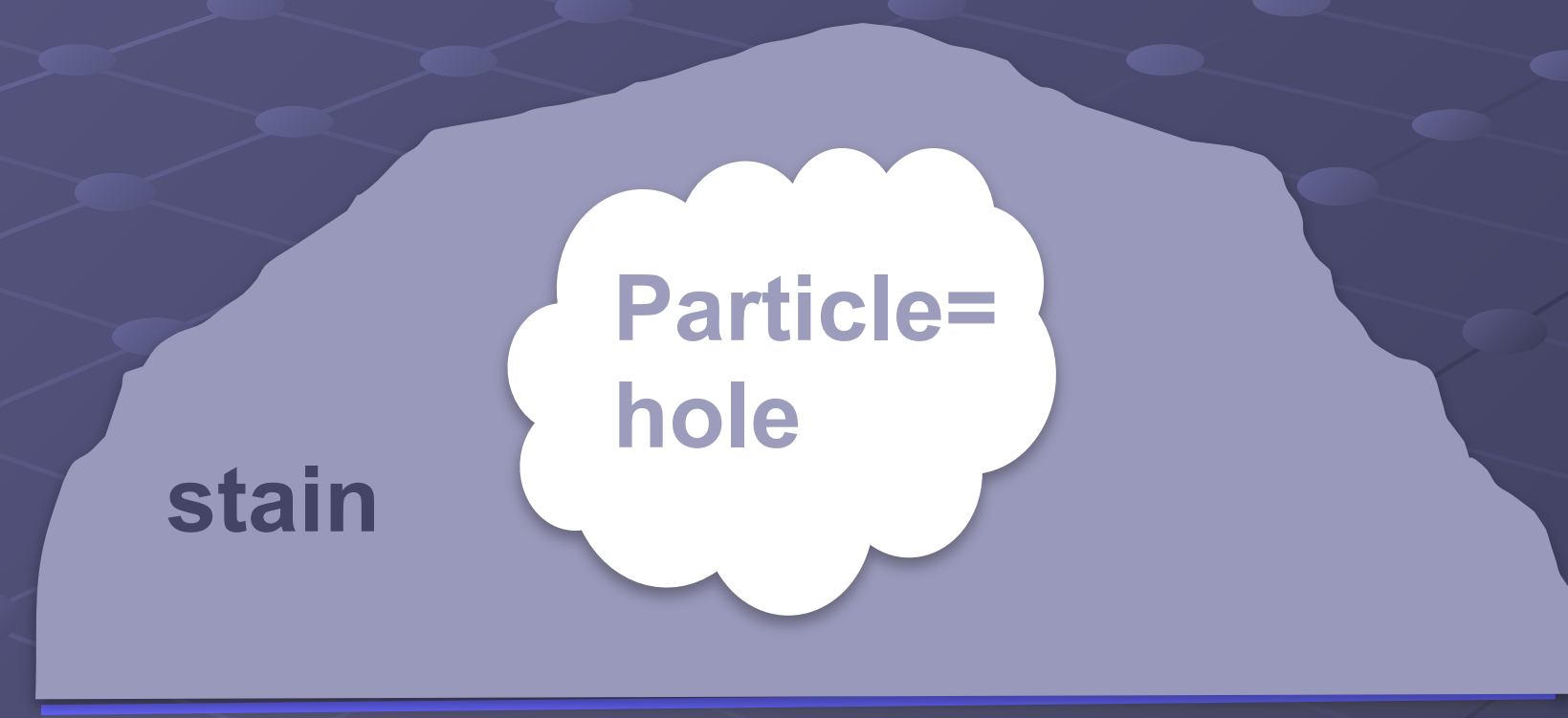
R.A. Crowther, L.A. Amos, J.T. Finch, D.J. DeRosier, & A. Klug, Nature 226, 421-425, 1970.

3D reconstruction was limited to molecular resolution by the negative stain.



Electron beam

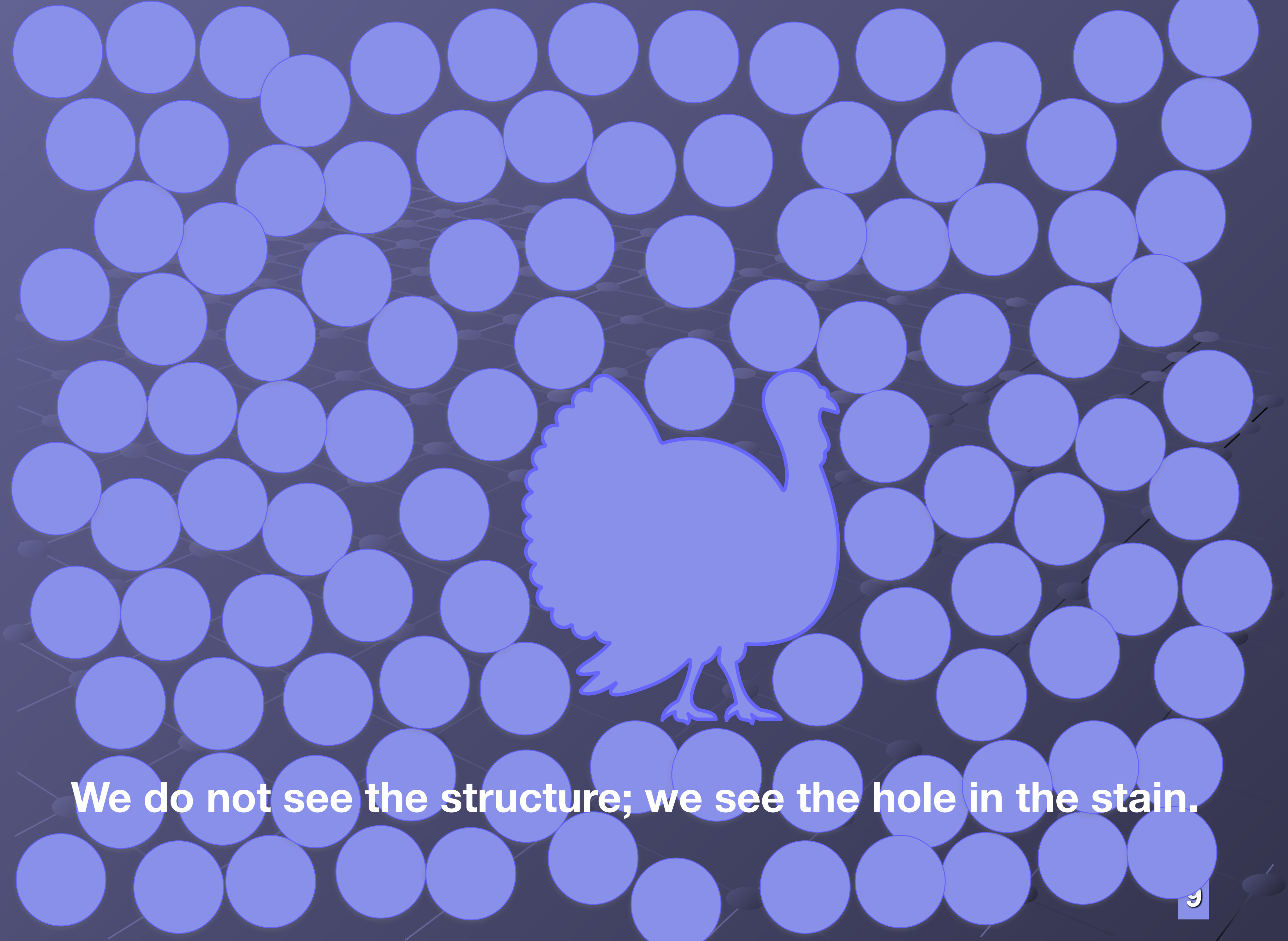
Uranium salts are good negative stains because they strongly scatter electrons providing amplitude contrast.



Number of electrons hitting image plane

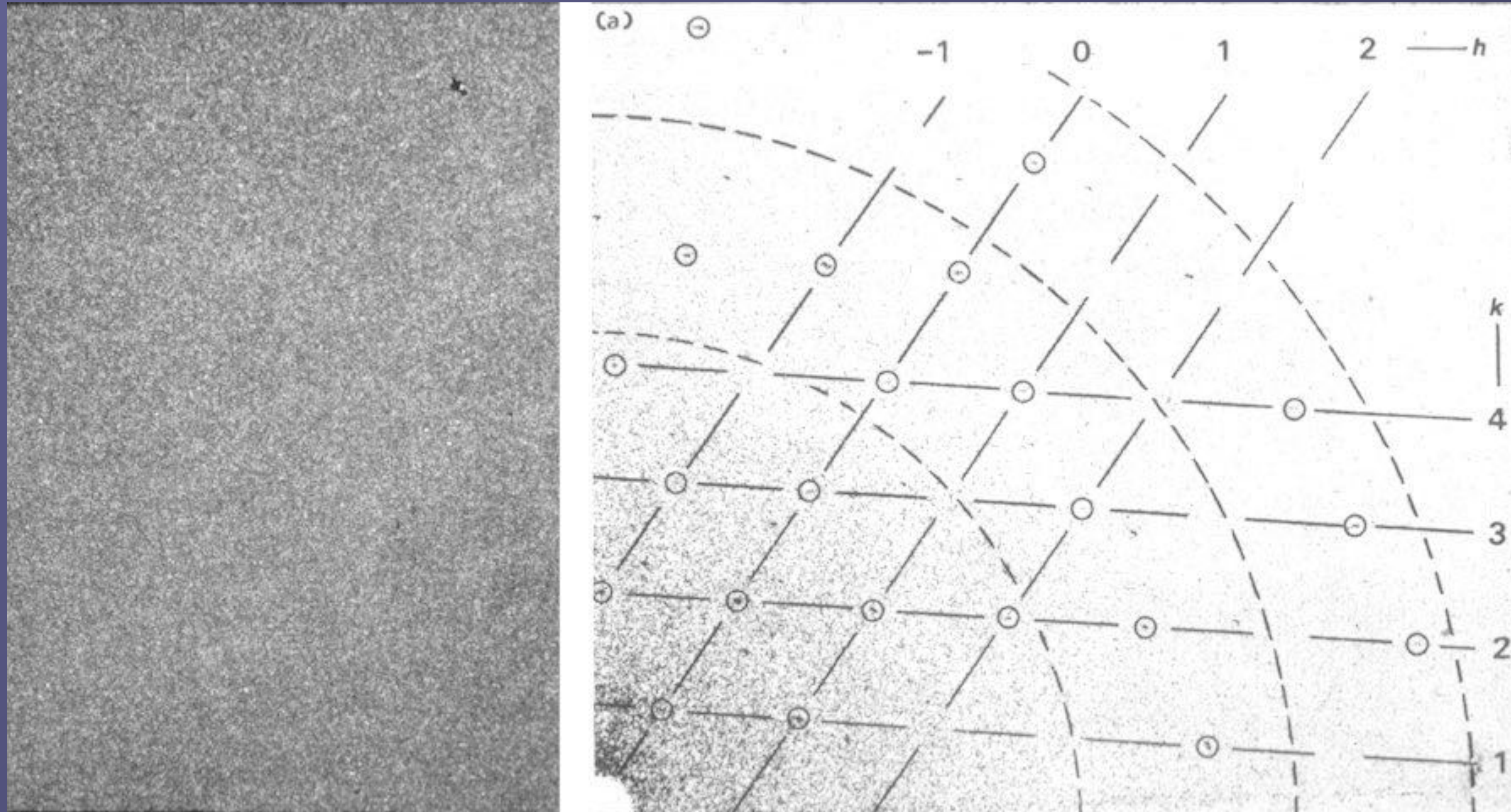


Stain occurs as clumps about 1 nm in size.



We do not see the structure; we see the hole in the stain.

Low dose EM image of a 2D crystal of bacterial rhodopsin bR - Unwin and Henderson, J Mol Biol. 1975 May 25;94(3):425-40



Fourier transform of image.

Negative stain was replaced by glucose with almost no contrast, but resolution is preserved to $\sim 7\text{\AA}$.

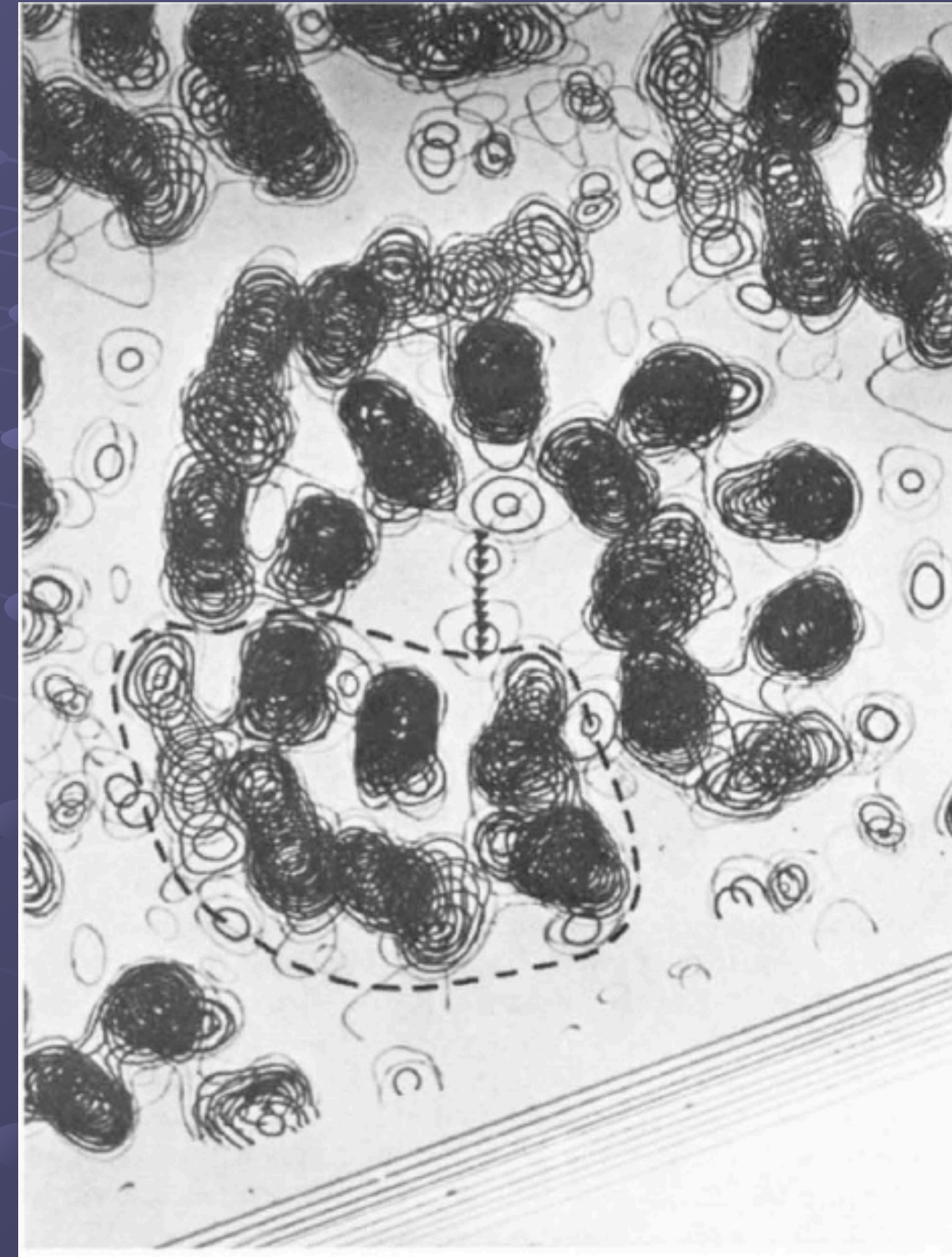
This was the first time we could see the protein itself instead of the hole it left in the negative stain.

This was the first 3D map of a membrane protein!



Nigel Unwin and Richard Henderson

Glucose was not a good embedding agent for single particles because the particles were 'hidden' by the glucose.



3D map of bR

Resolution = 7 Å

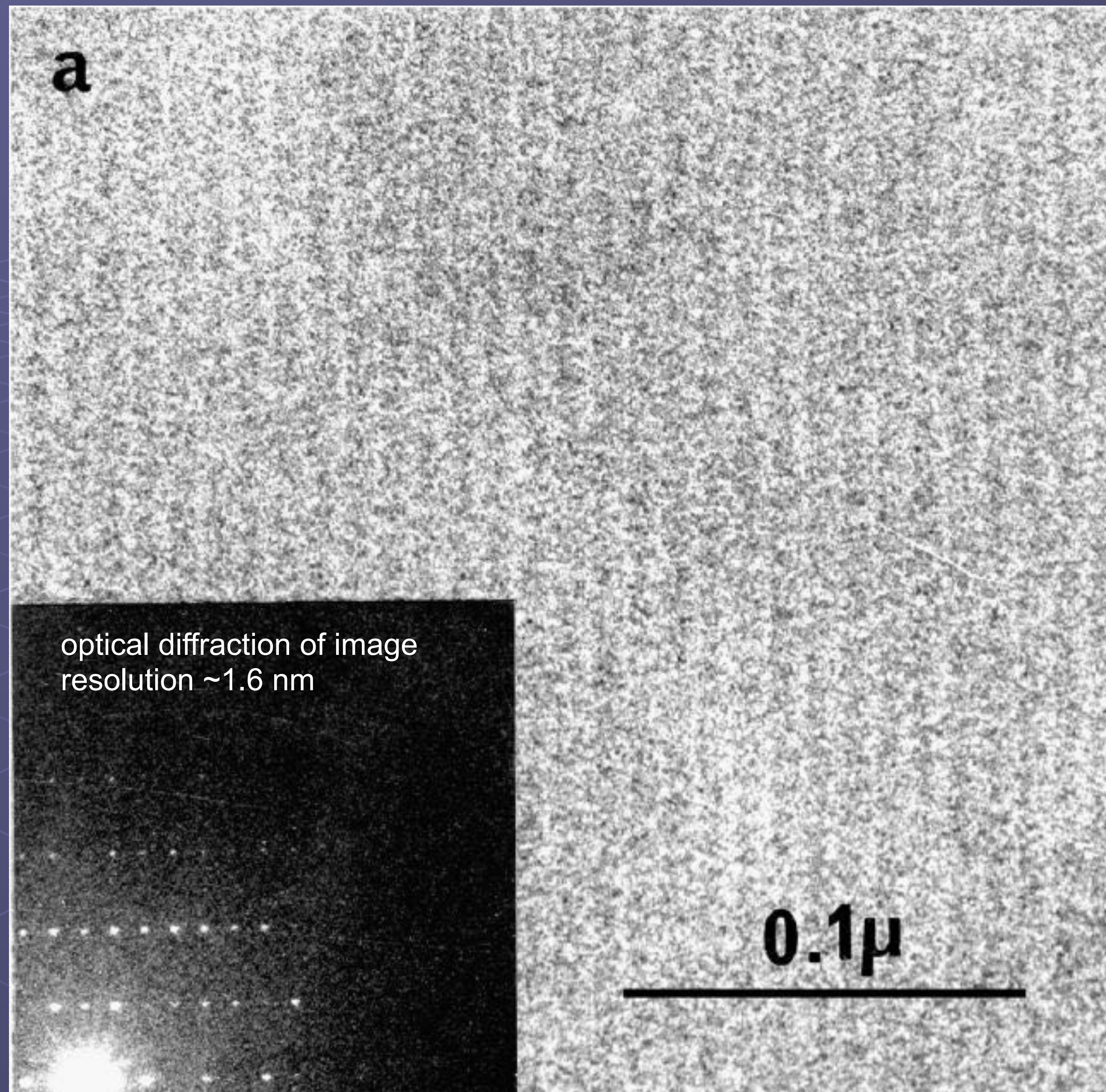
Ice is a better embedding agent than glucose because there is contrast.



Bob Glaeser



Ken Taylor

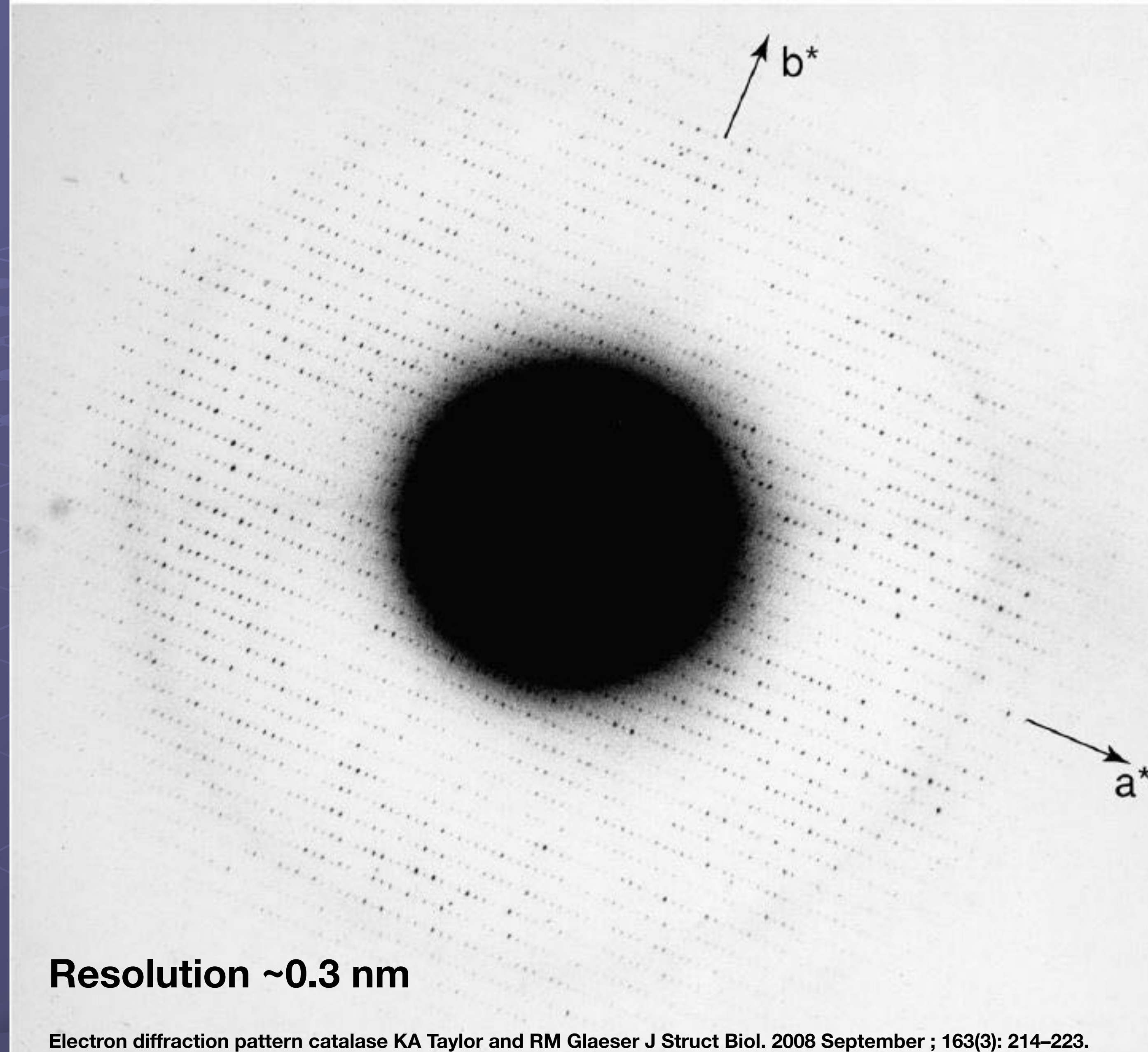


Frozen-hydrated specimens

Thin crystal of catalase in ice

Was the preservation of structural detail only as good as negative stain i.e., 16 Å?

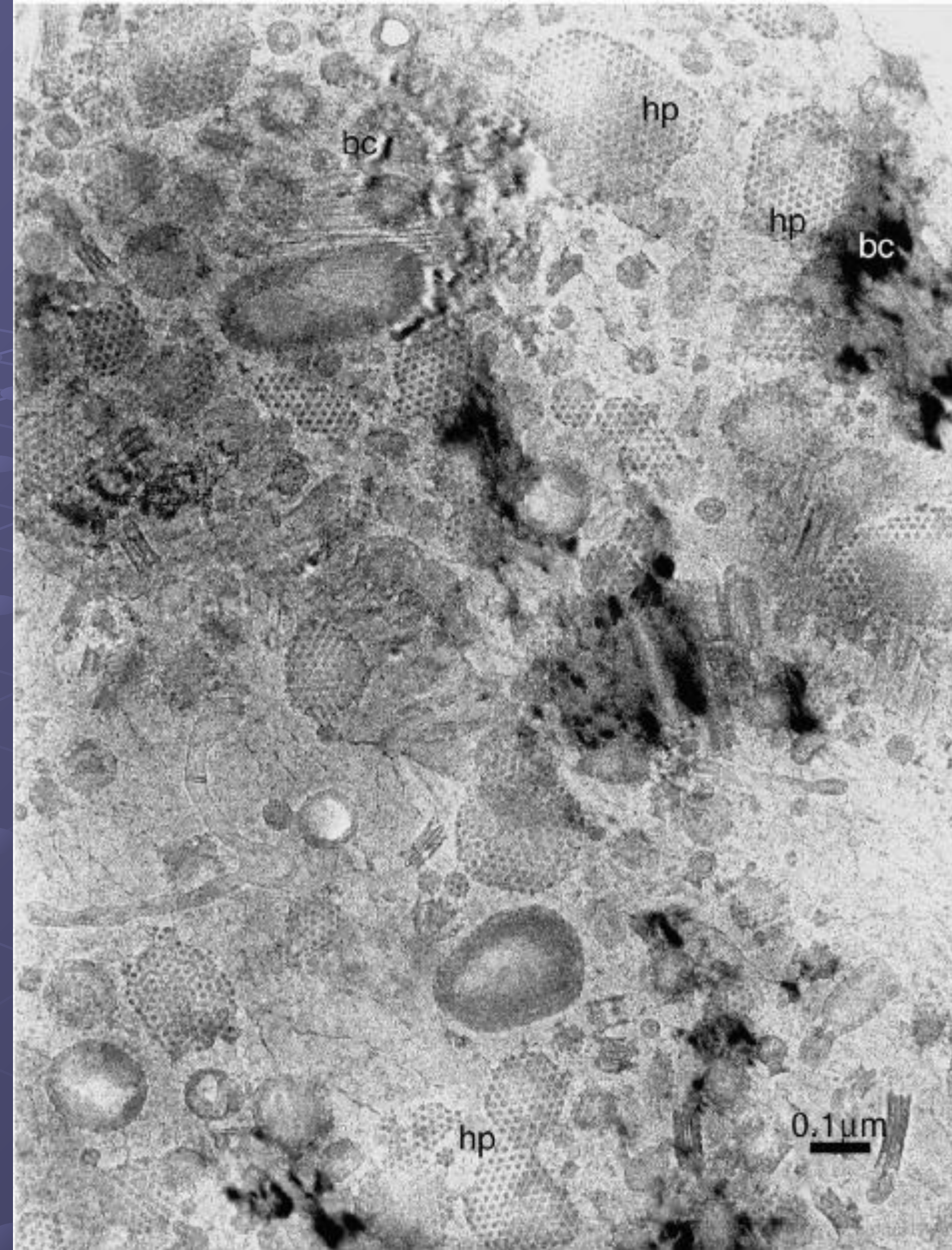
Electron diffraction pattern shows preservation is good to near atomic resolution.



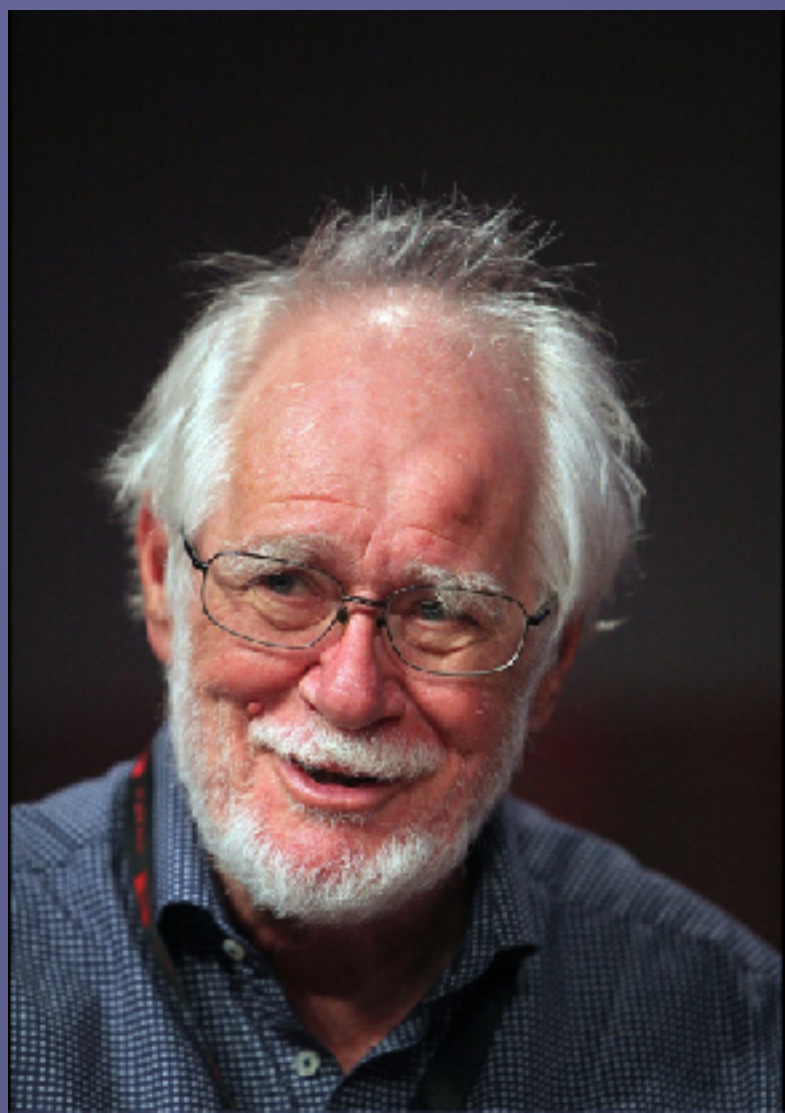
Frozen-hydrated cell wall material from *Spirillum serpens*

The good news: frozen water embedding make particles visible.

The bad news: ice crystals alter contrast and they disrupt structures.



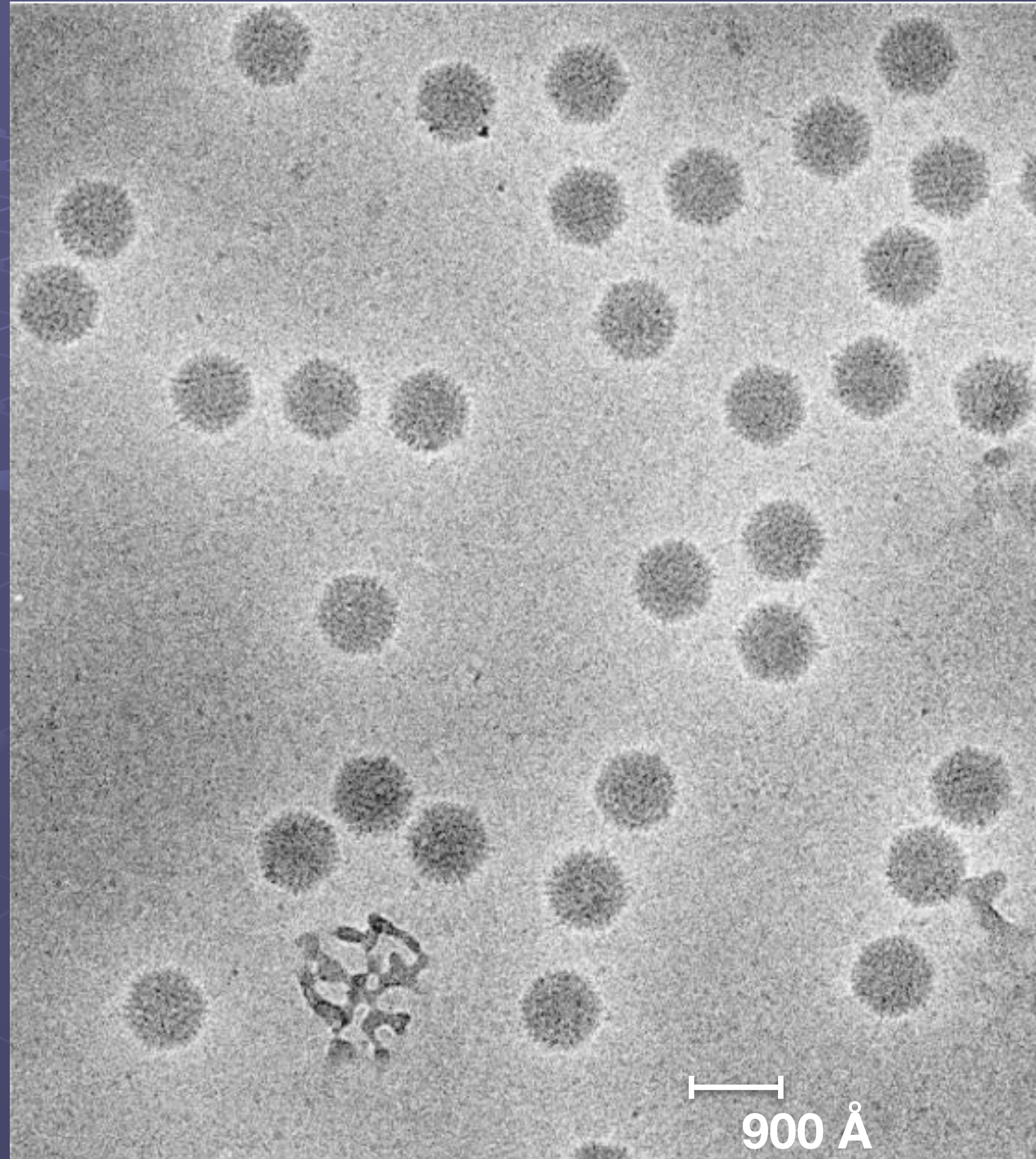
bc = bend contour, which shows the ice is crystalline



Jacques Dubochet

Plunge freezing into liquid ethane ($T < -140$ C) produces vitreous as opposed to crystalline ice.

Adenovirus in amorphous (vitreous) ice

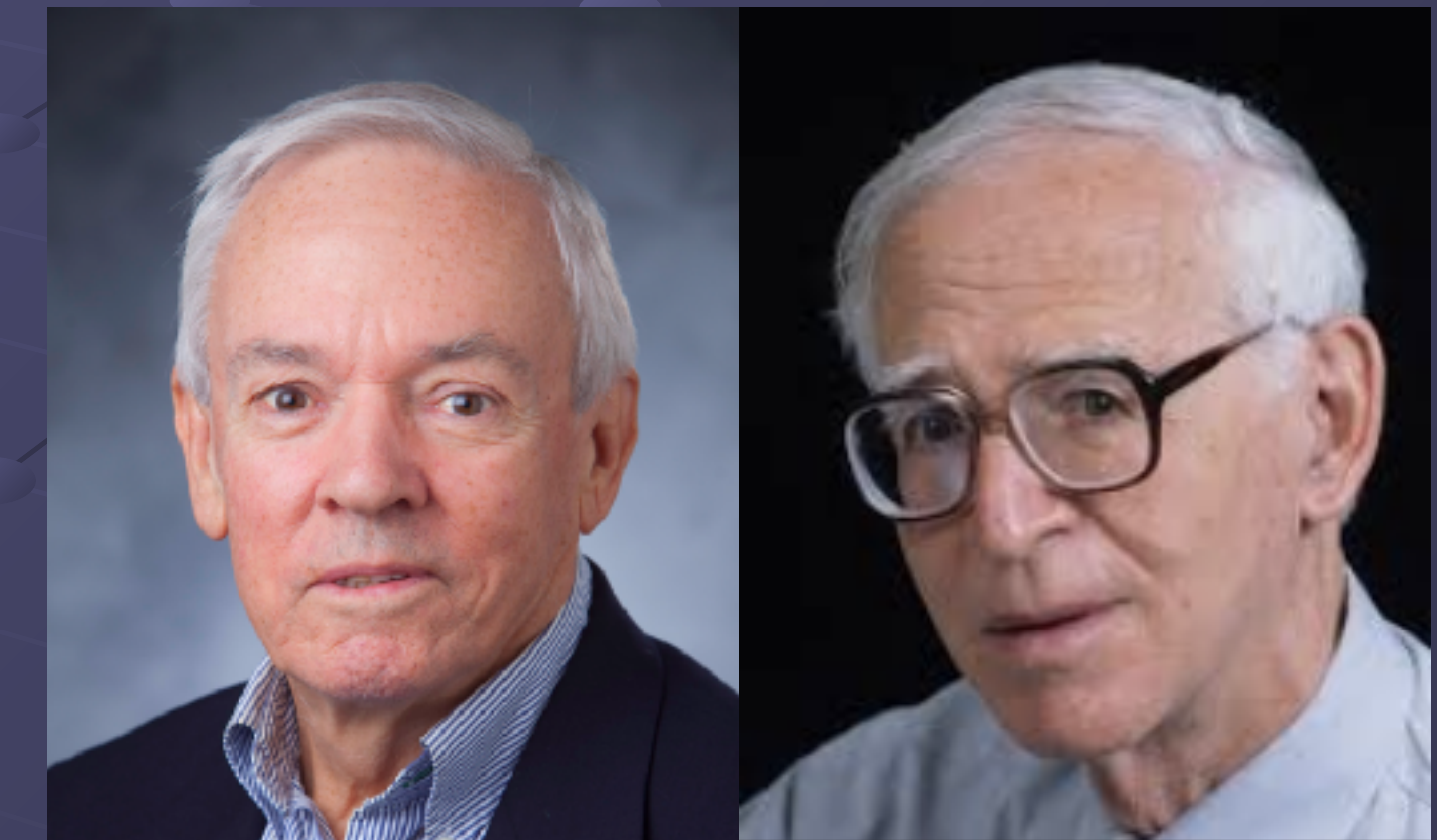
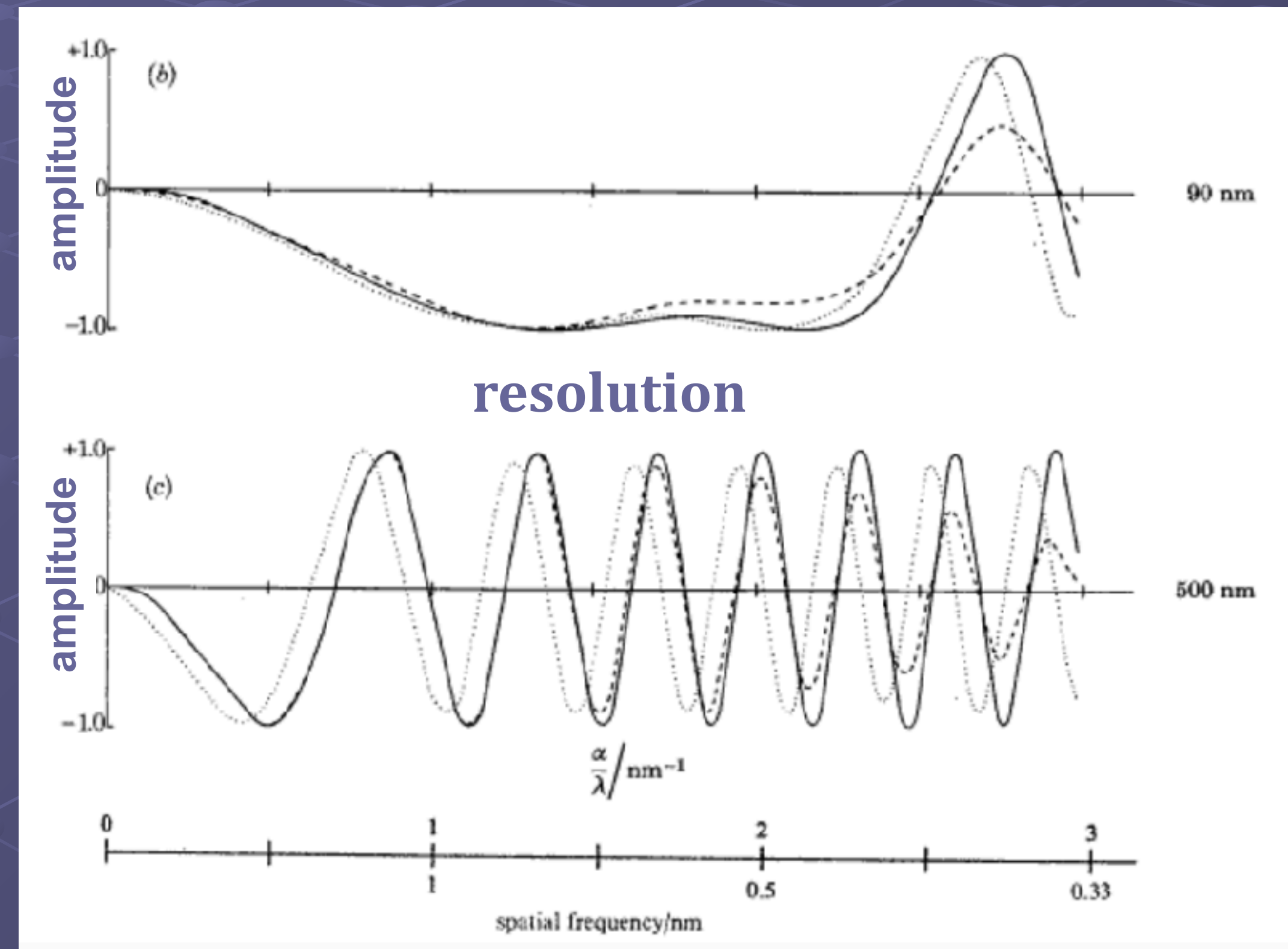


Particles in vitreous ice are transparent: no contrast!

Defocussing produces phase contrast but it alters the information in the image.

Erickson and Klug showed how the Fourier transform of the image is altered by defocus and how to correct for it.

Contrast transfer function or CTF

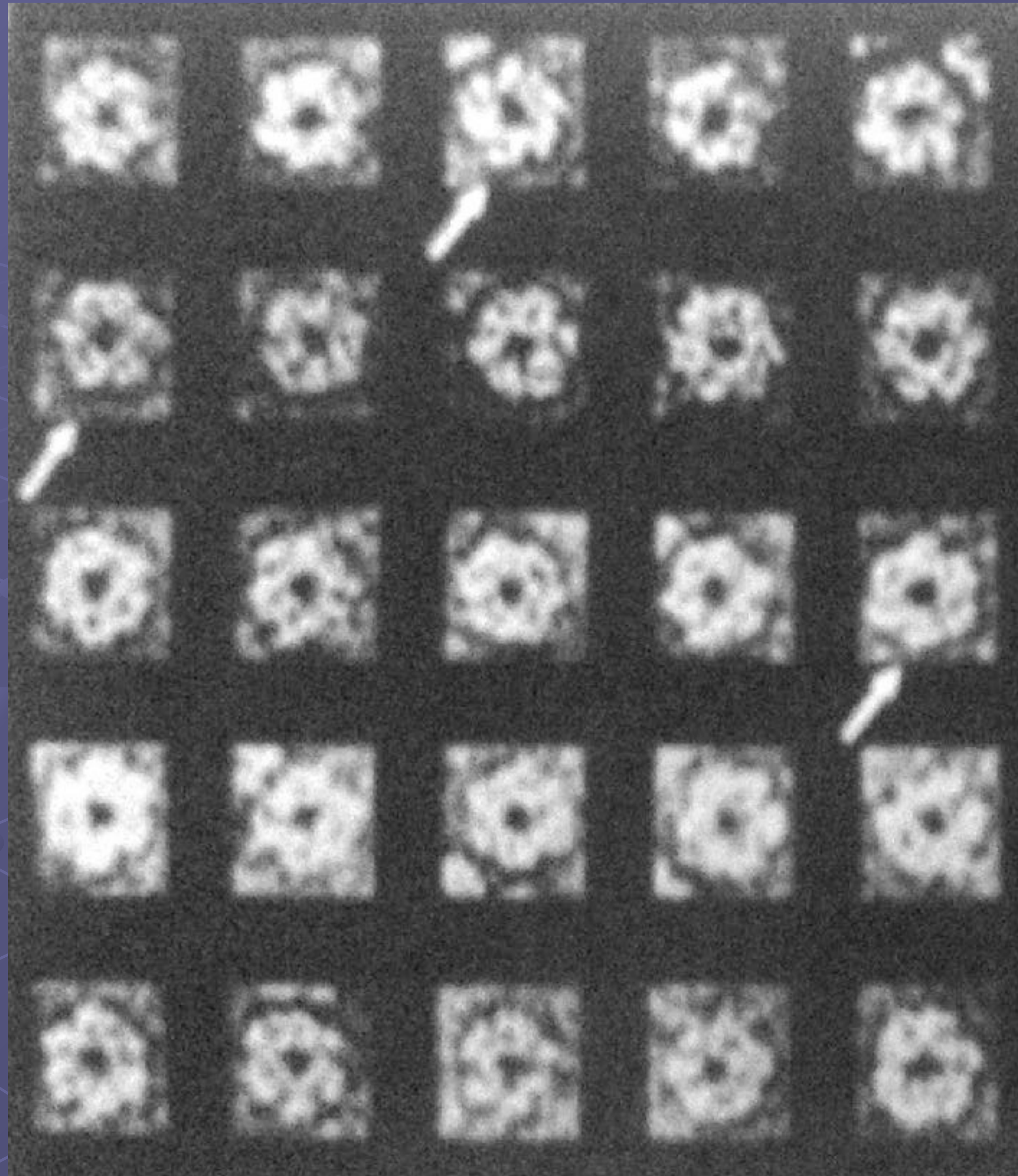


Harold Erickson

Aaron Klug

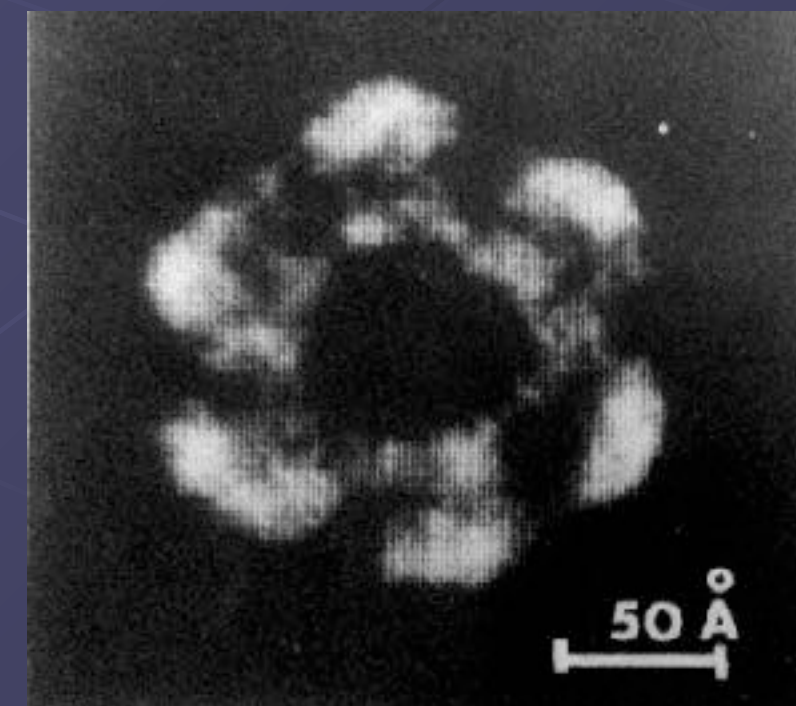
H. P. Erickson and Aaron Klug. Measurement and compensation of defocusing and aberrations by Fourier processing of electron micrographs Phil Trans Roy Soc Lond B Volume 261 Issue 837 p 105-118 , 1971.

single particle analysis

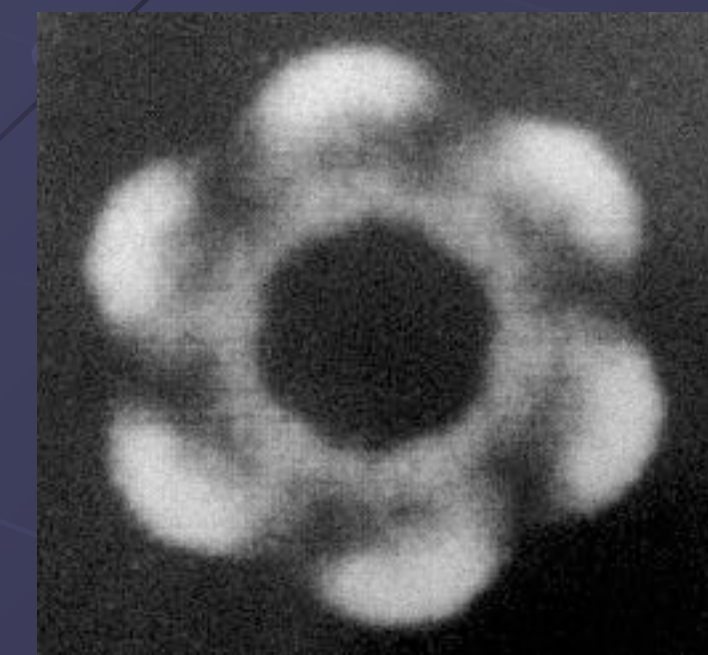


Joachim Frank

Averaged
image



Rotationally
averaged



Frank, J., Goldfarb, W., Eisenberg, D., and Baker, T.S. (1978). Reconstruction of glutamine synthetase using computer averaging. *Ultramicroscopy* 3, 283-290.

Multivariate statistics introduced by Frank and van Heel allowed them to sort particle images into classes and produce class averages.

Class averages can sort images by orientation, conformation, and composition!

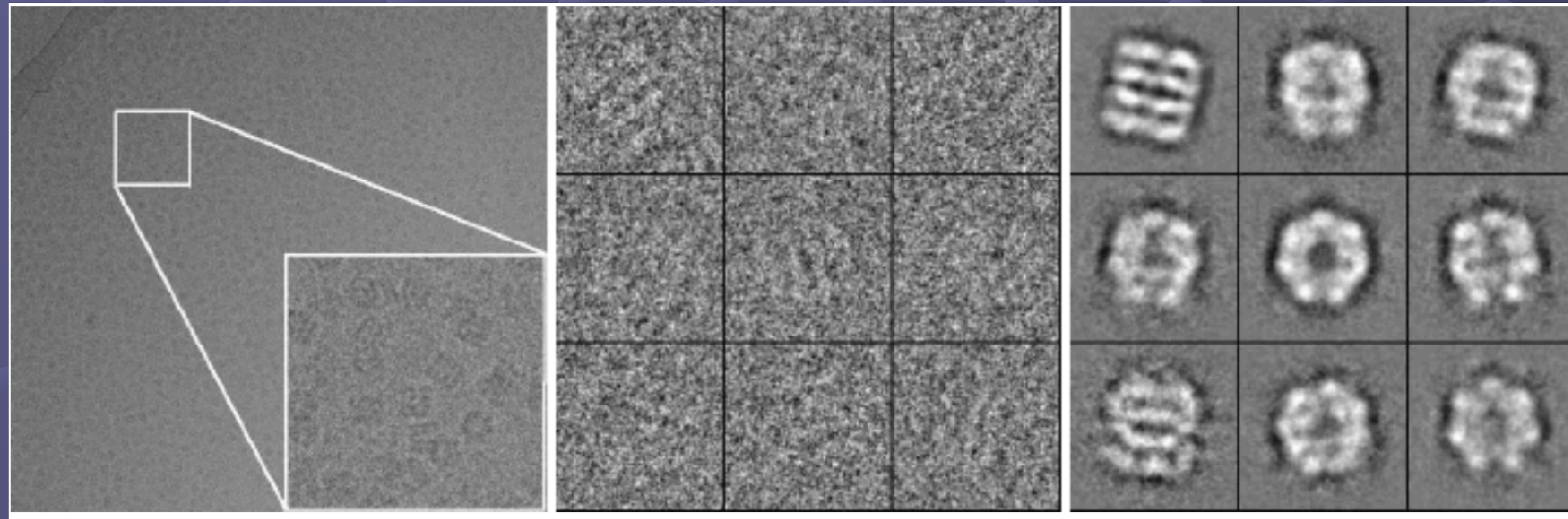


Joachim Frank



Marin van Heel

van Heel M, Frank J. Use of multivariate statistics in analysing the images of biological macromolecules. *Ultramicroscopy*. 1981;6(2):187-94.



Cryo EM image

Particle images cut out from micrograph

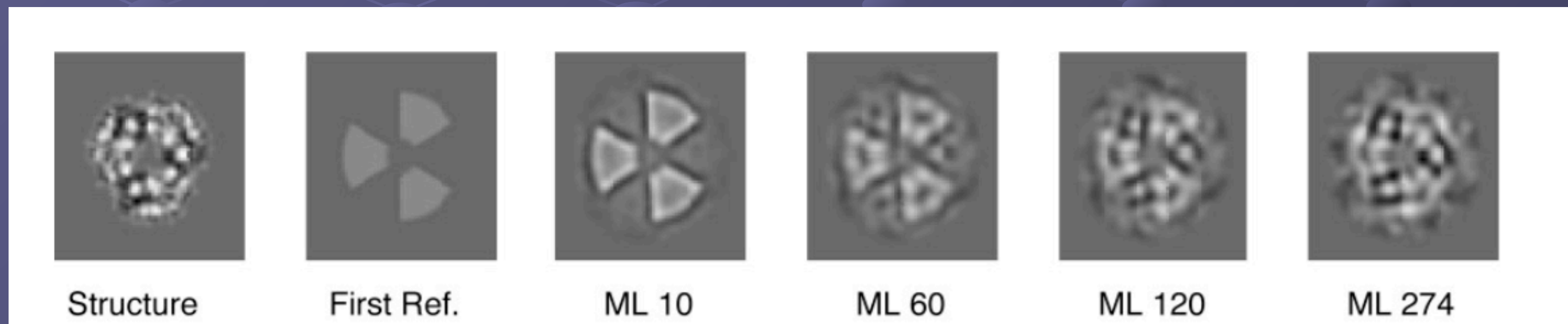
average of images in each class

Maximum-likelihood

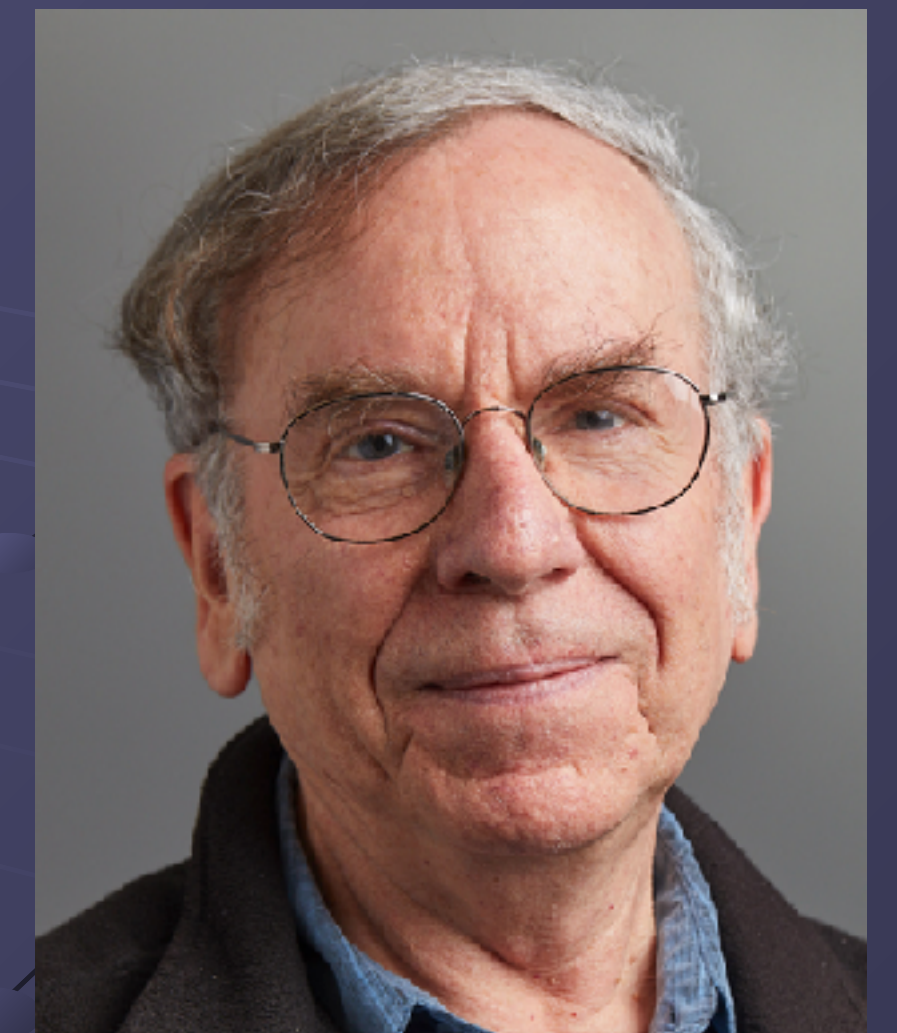
Particles are put into classes for averaging weighted by the probability they belong to that class.



Cross correlation



Maximum-likelihood



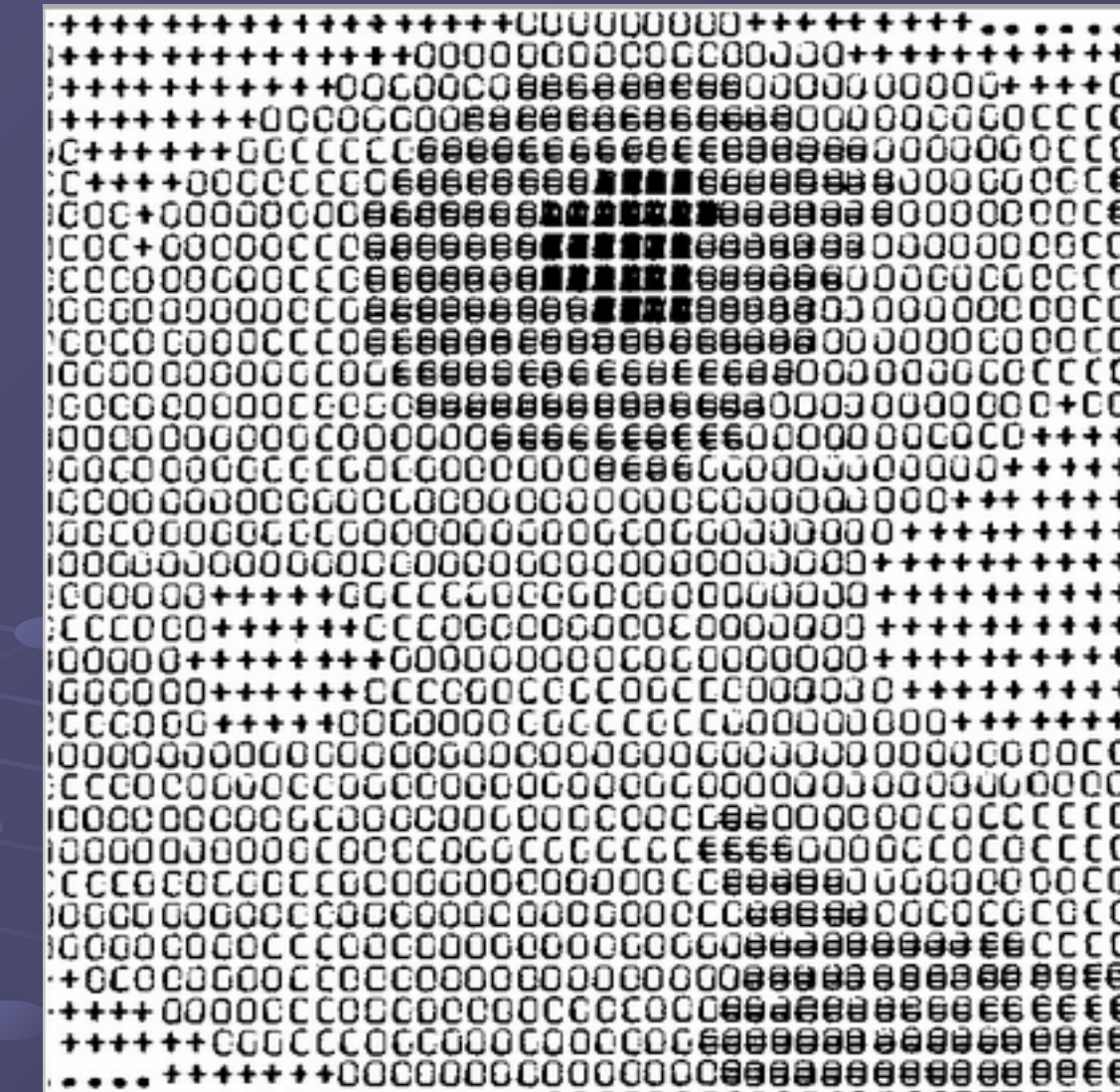
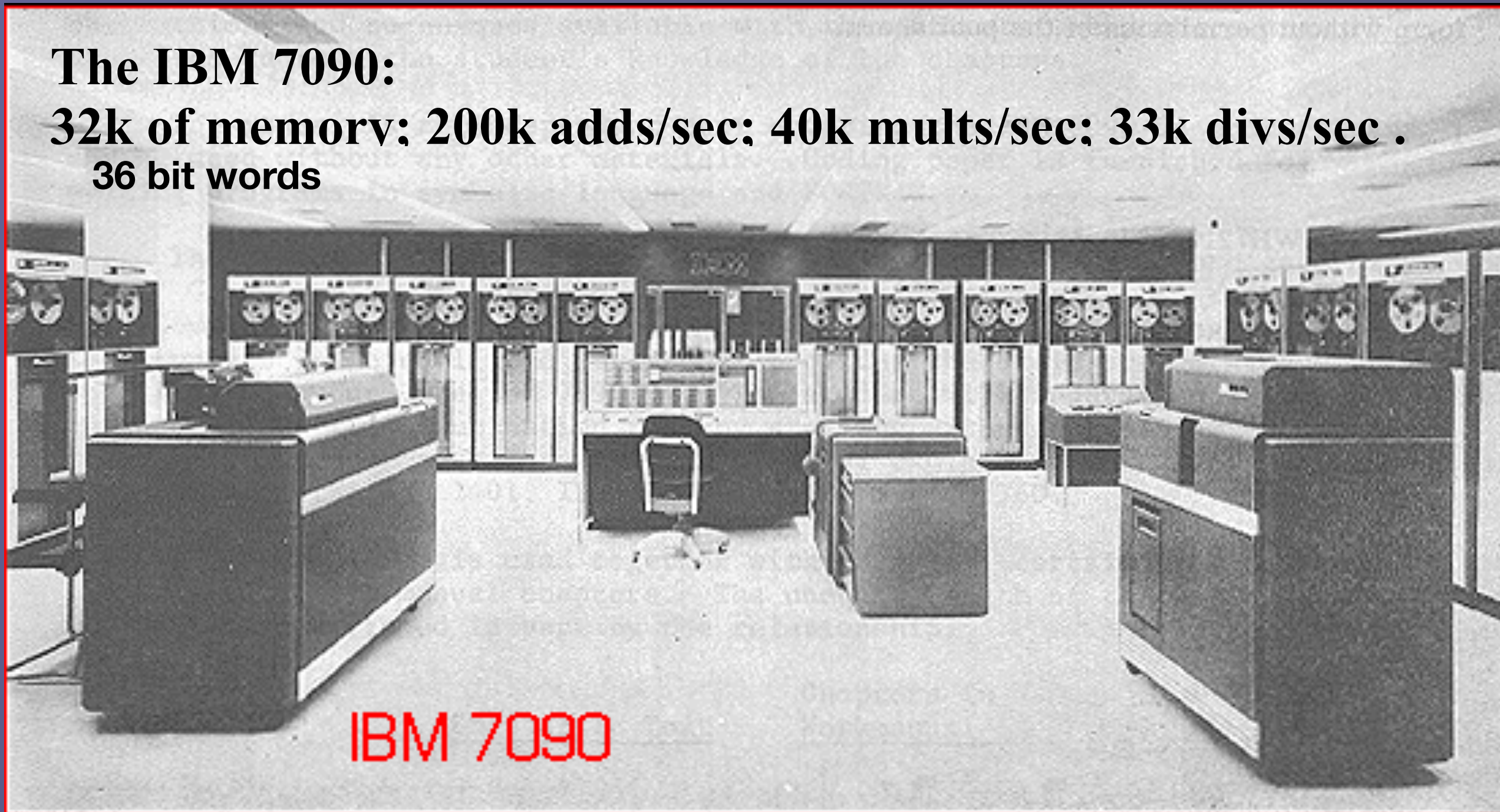
Fred Sigworth

Maximum-likelihood prevents iterative alignment and sorting from falling into local minima.

An obvious important development: faster computers with more memory and graphics.

The IBM 7090:

32k of memory; 200k adds/sec; 40k mults/sec; 33k divs/sec .
36 bit words



<http://employees.oneonta.edu/baumanpr/geosat2/RS%20History%201960-2000/RS-History-1960-2000.htm>

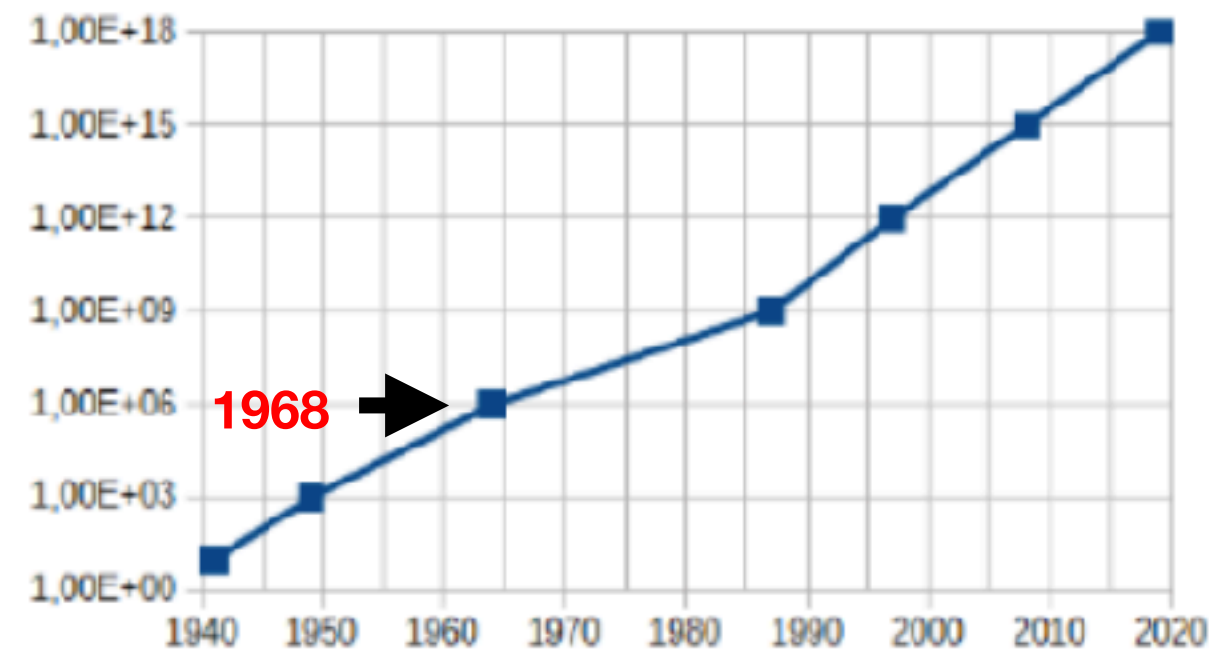
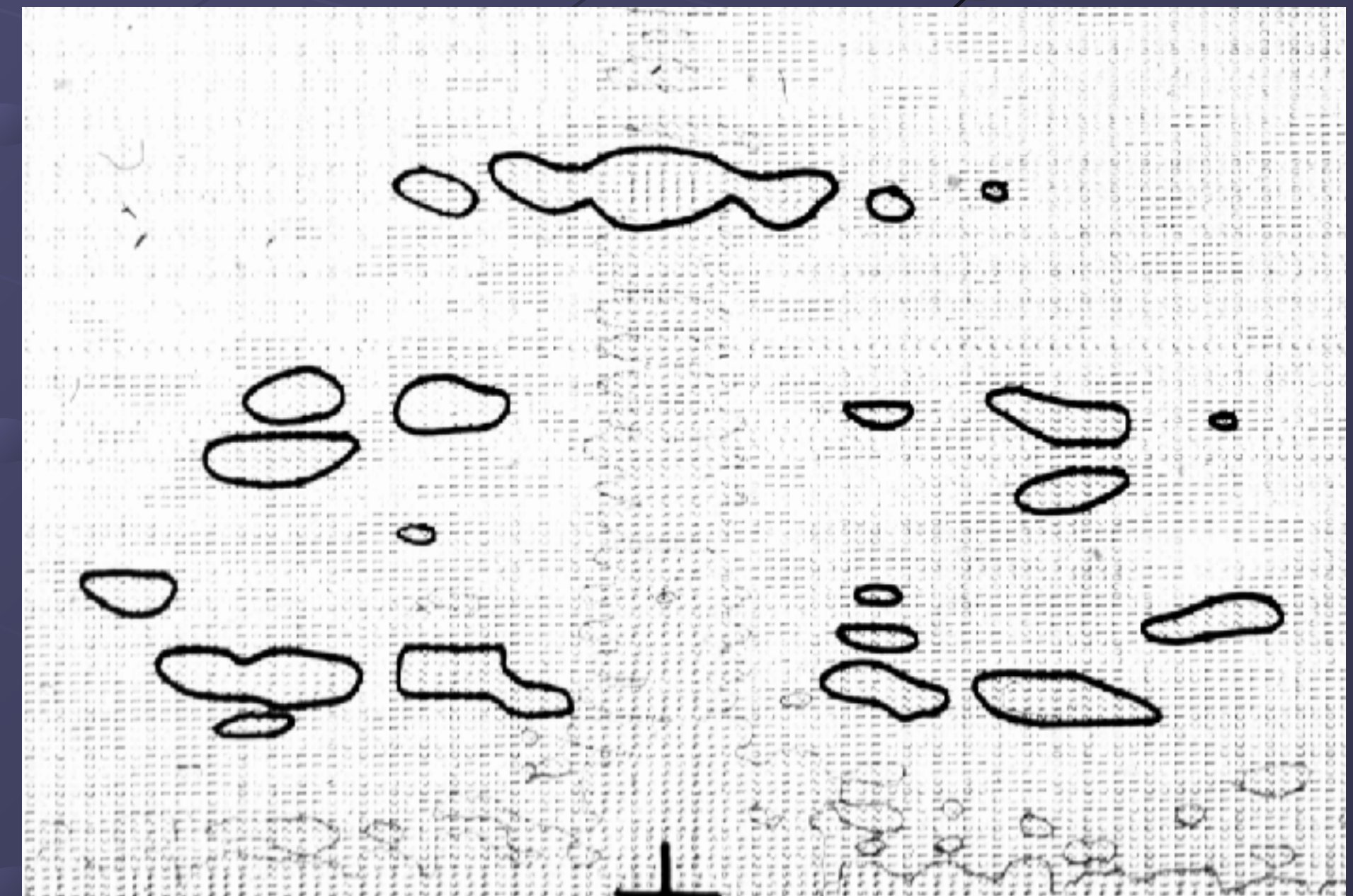


Figure 1: Computer Performance Evolution Over Time (FLOPs)



Many, many improvements in software since Joachim Frank's SPIDER software package of 1978

**There are many software packages available to use singly or in series.
AI/ML is being used more in these packages.**

Improvements in the electron microscope.

Built-in stable cryo grid holders

Higher voltage, which is good for thicker specimens but probably not for very thin ones.

Field emission guns with better coherence dropped structural resolution to about 4 Å.

Direct electron detectors with speed and sensitivity further improved resolution to 2Å and better.

Energy filters removed inelastically scattered electrons from the images of thicker samples.

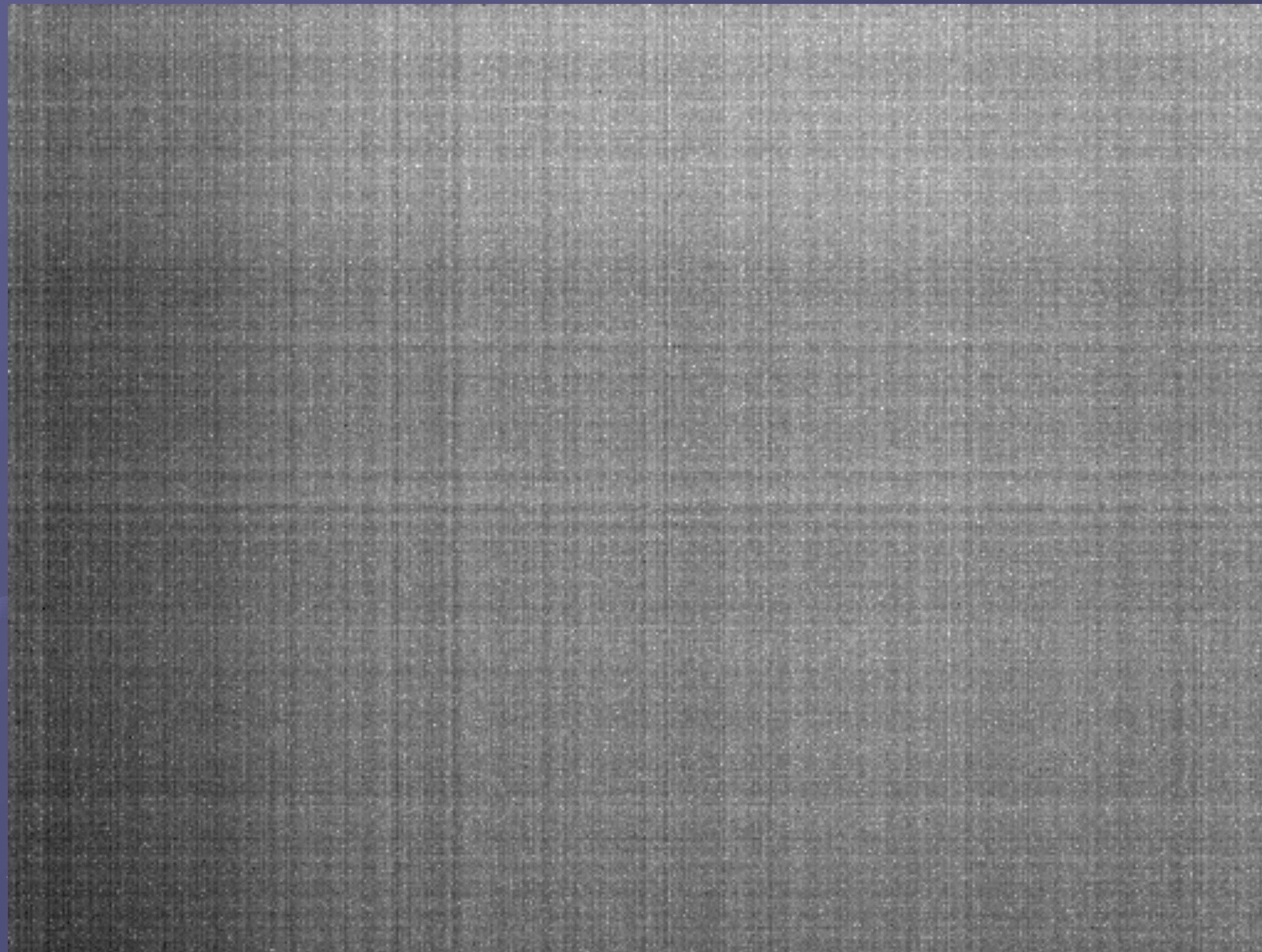


<https://collection.sciencemuseumgroup.org.uk/objects/co8648182/main-component-of-siemens-elmiskop-1-electron-microscope-electron-microscope>

<https://www.thermofisher.com/us/en/home/electron-microscopy/products/transmission-electron-microscopes/krios-g4-cryo-tem.html>

Beam induced motion and/or drift cause loss of resolution preventing resolutions below 4Å.

The direct electron detectors made it possible to break a single exposure into a movie of many frames and correct for the motion.



**Recorded with
direct electron
detector DE-12
(Direct Electron)**

Frame rate = 40 fps

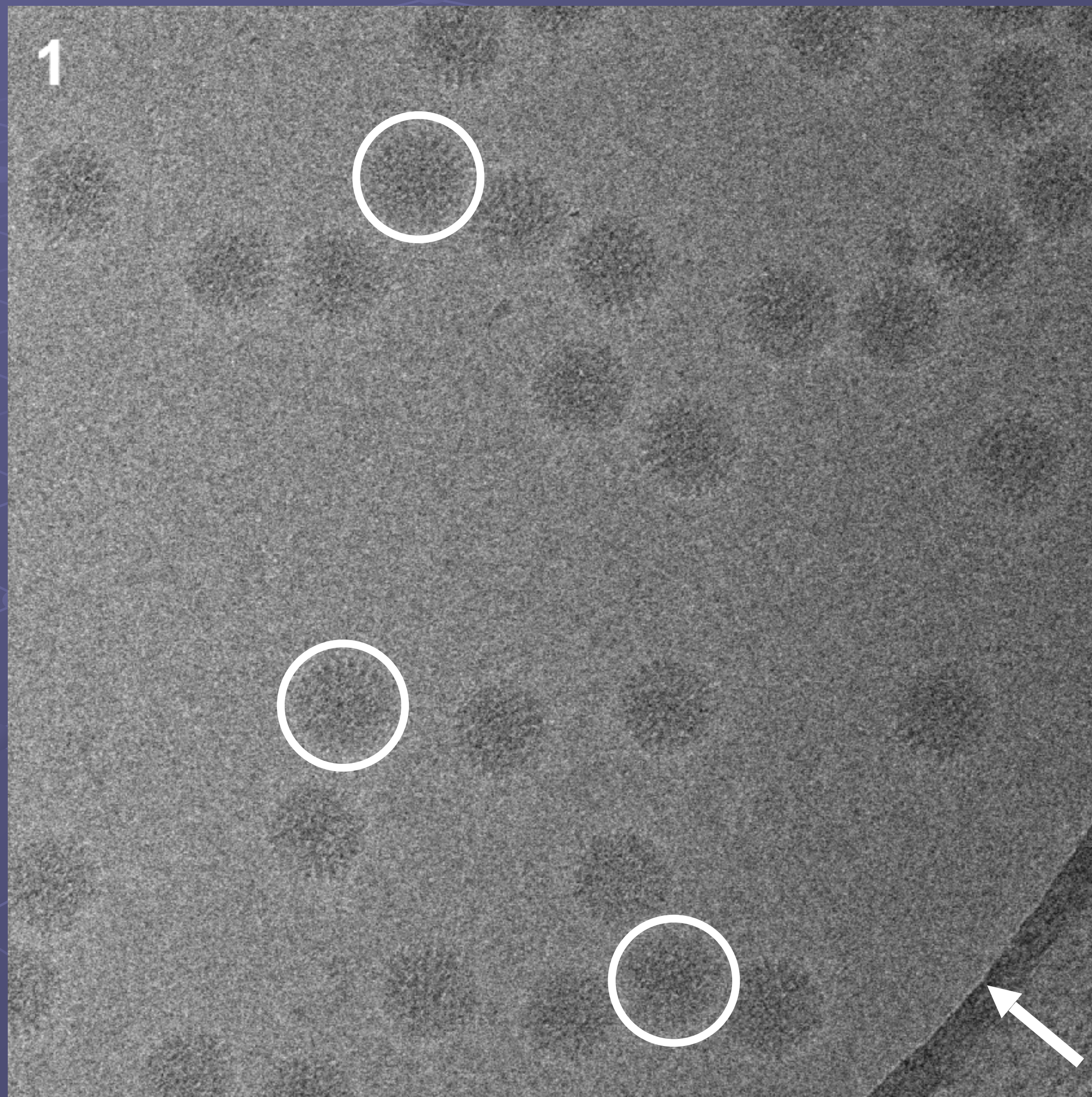
Dose/frame = 0.5 e-/Å²

Duration = 1.5 s

No. of frames = 60

Total dose = 30 e-/Å²

10-Frame Averages

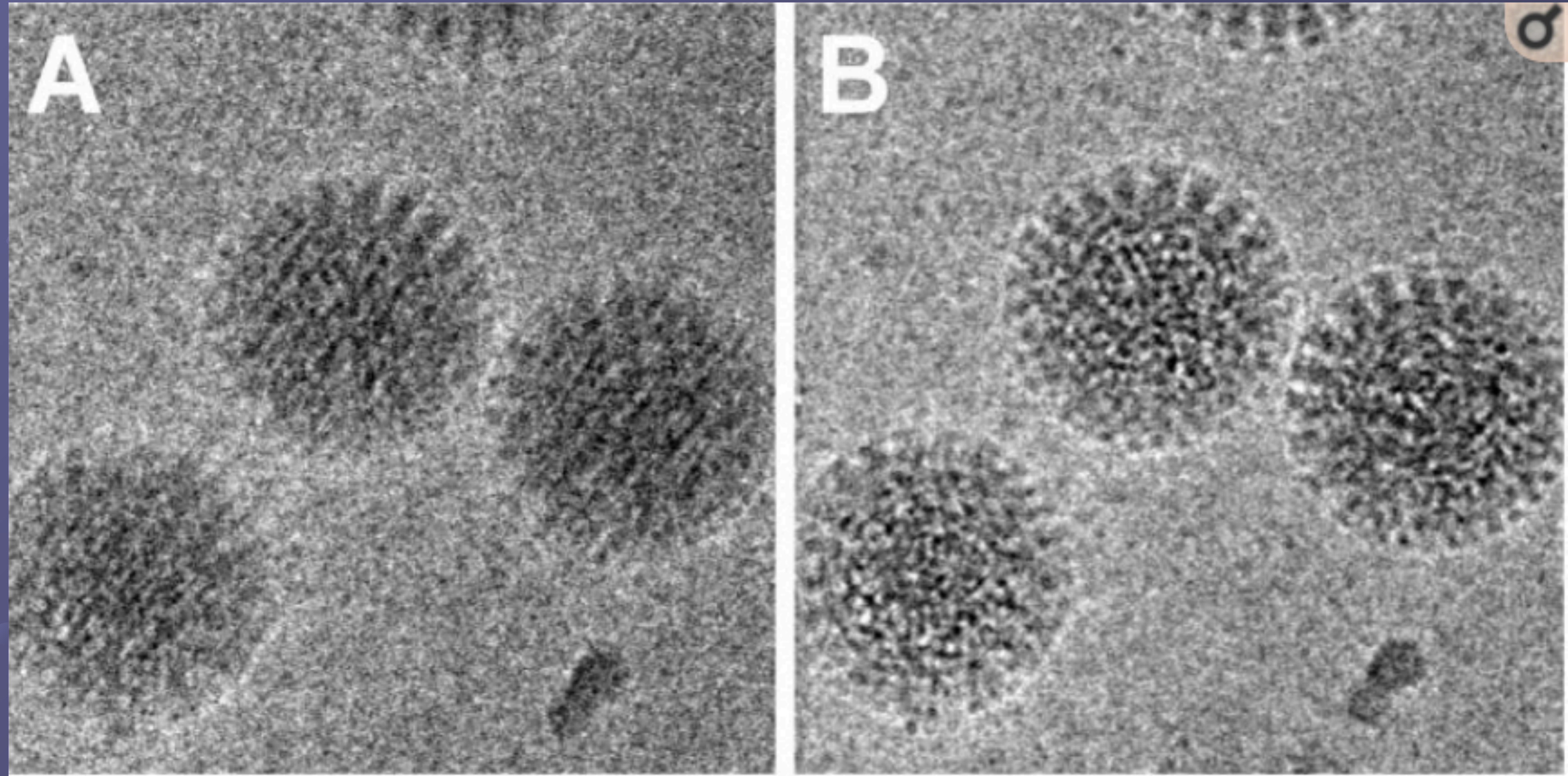


Each averaged frame
corresponds to 0.25 s.

Dose/frame = $5 \text{ e}^-/\text{\AA}^2$

Uncorrected for motion

Corrected for motion

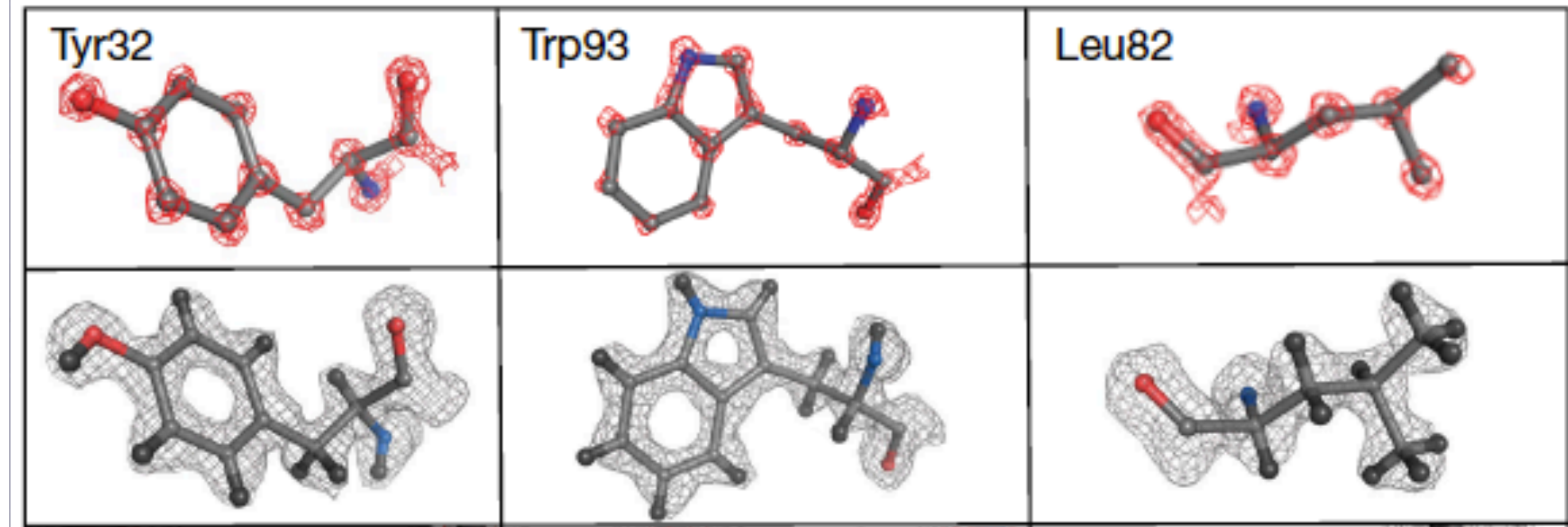
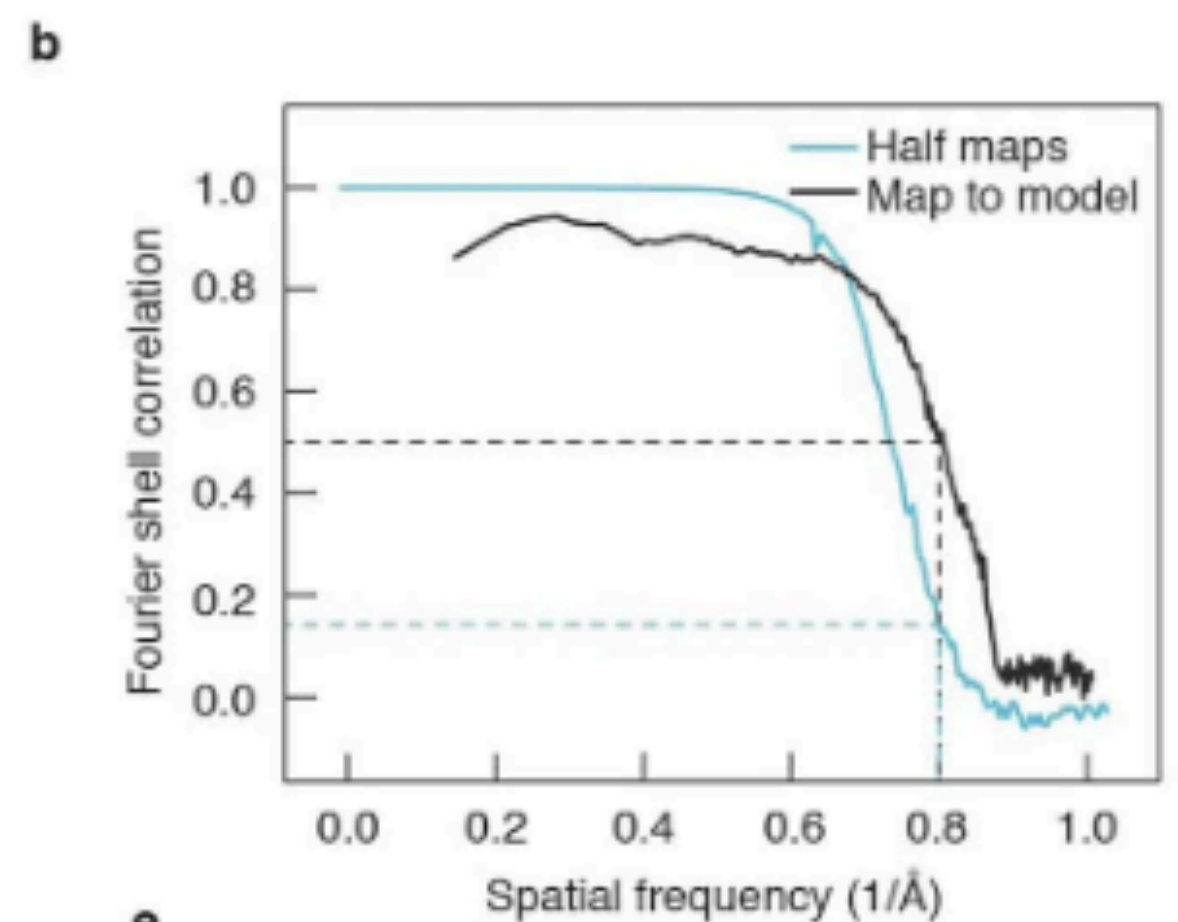
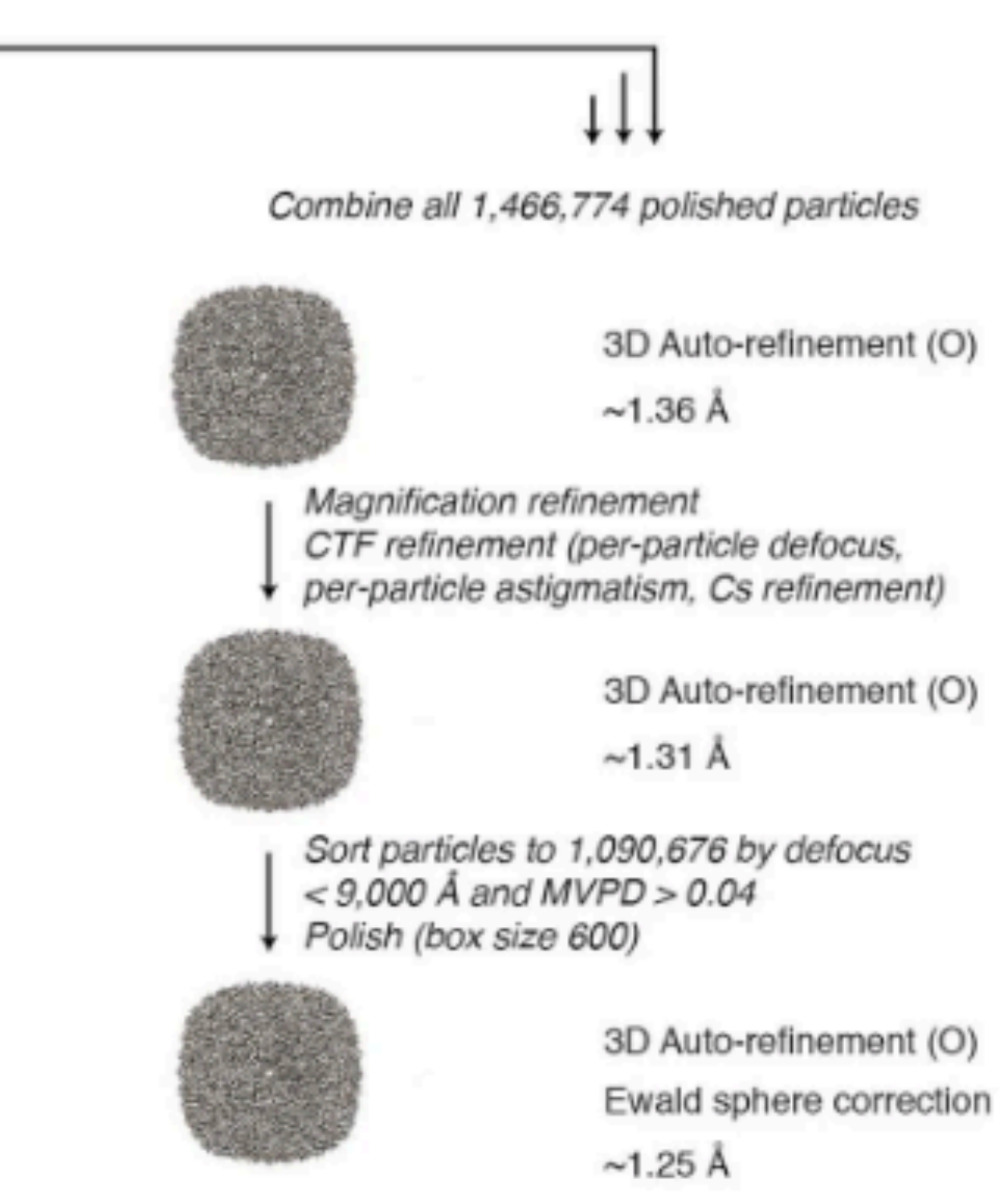
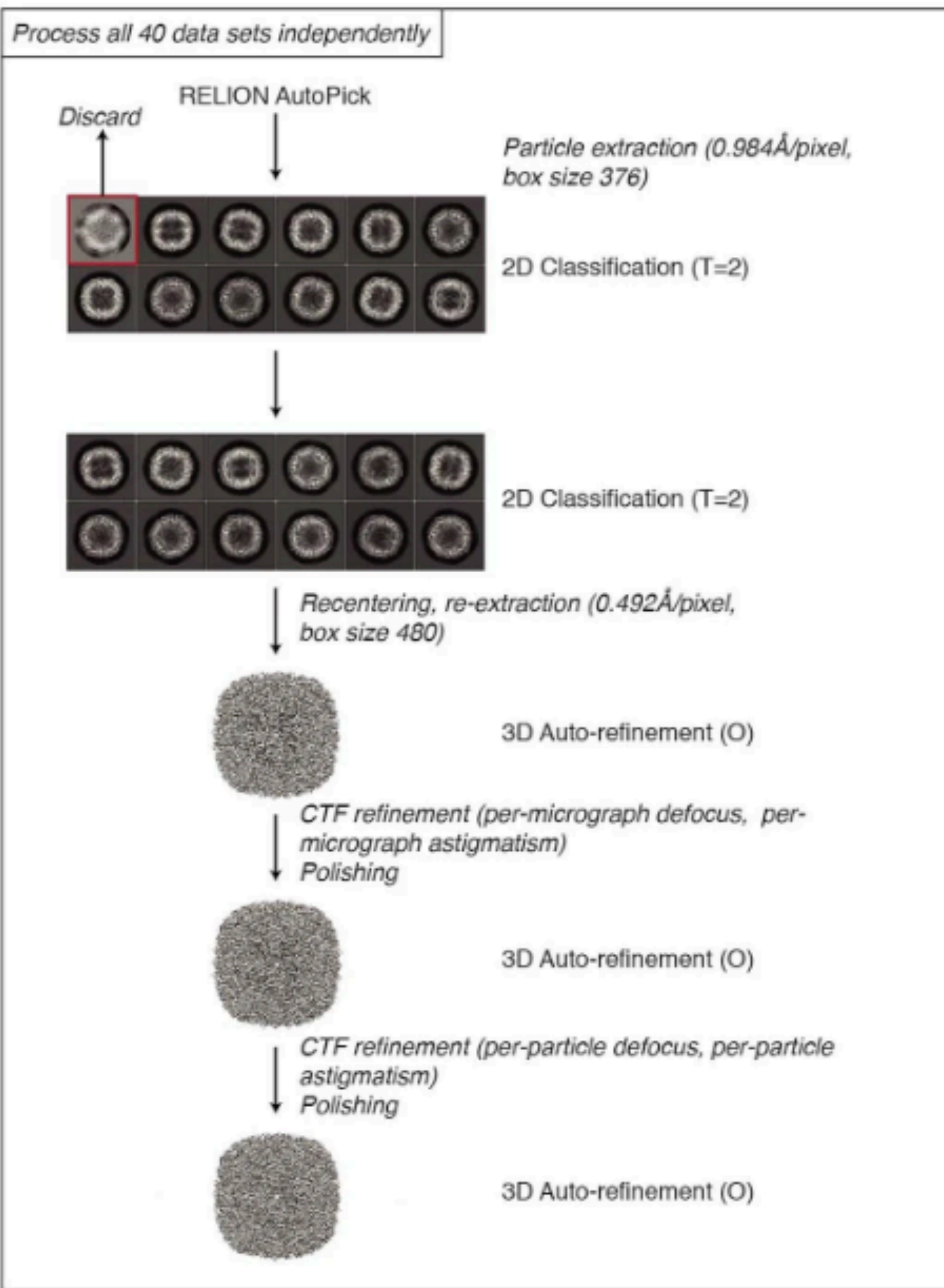


The direct electron detectors has all but eliminated the deleterious effects of BIM.

We have covered the key advances in single particle cryo-EM.

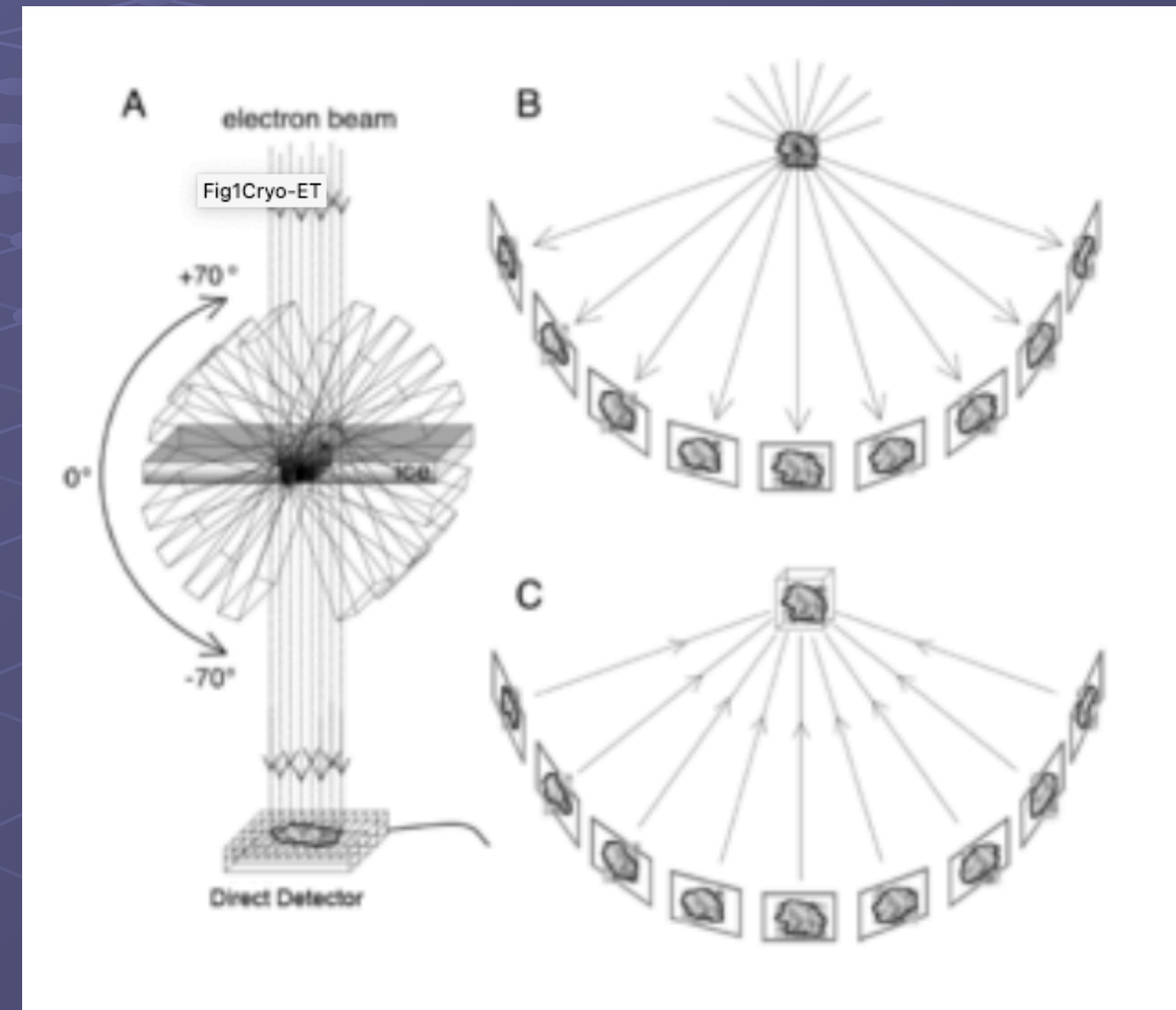
25

The resolution revolution's best: a 1.25 Å resolution map of apoferritin



Cryo electron tomography

We turn from looking at single particles to looking at cells or organelles.

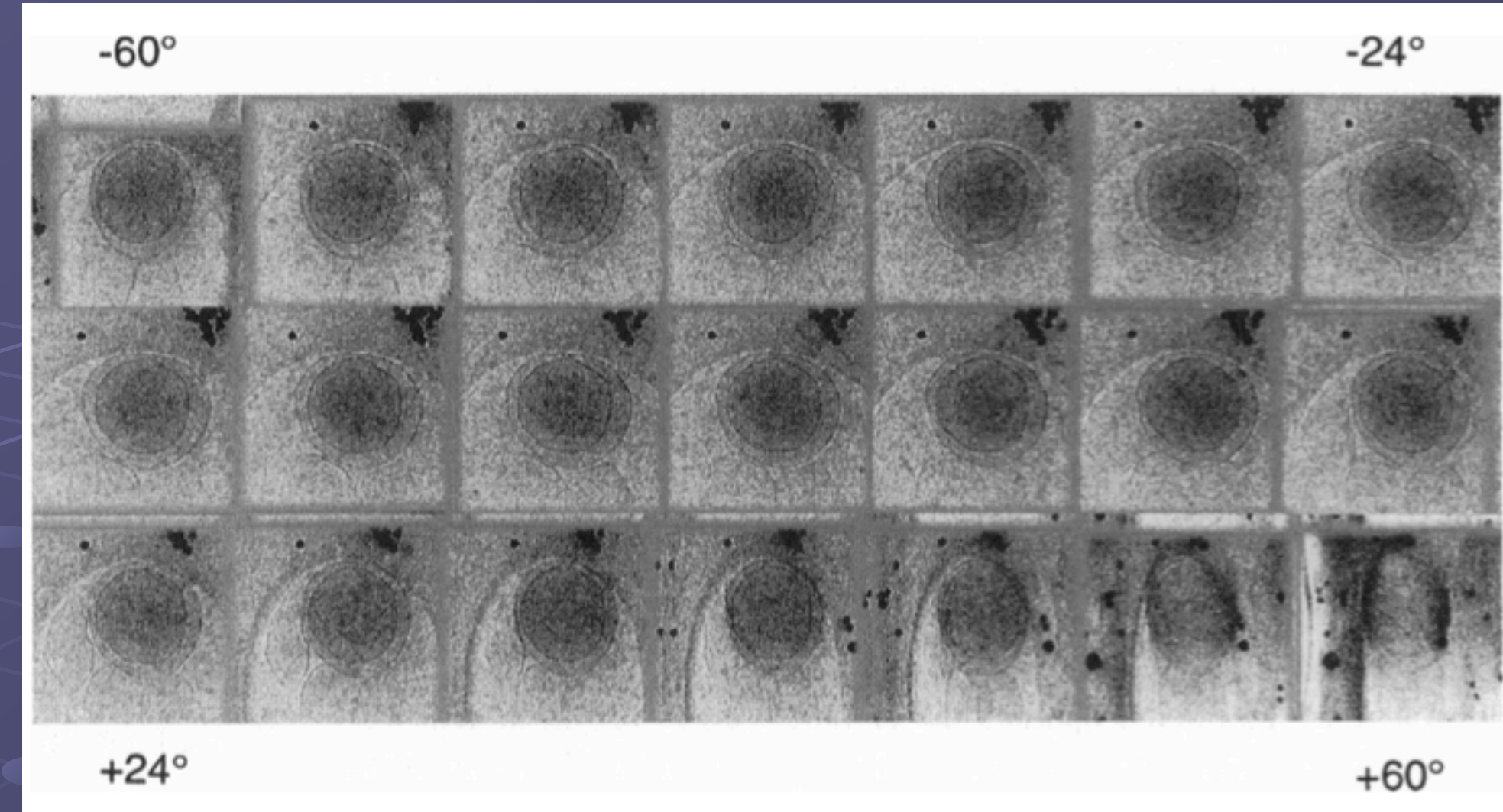


(Steven and Belnap, Current Protocols in Protein Science, 2005).

Where in the cell are the single particle structures we have solved and with which other cellular structures do they interact?

Cryo-ET of lipid vesicles in 1995

Tilt series



Wolfgang Baumeister

Slice from the tomogram

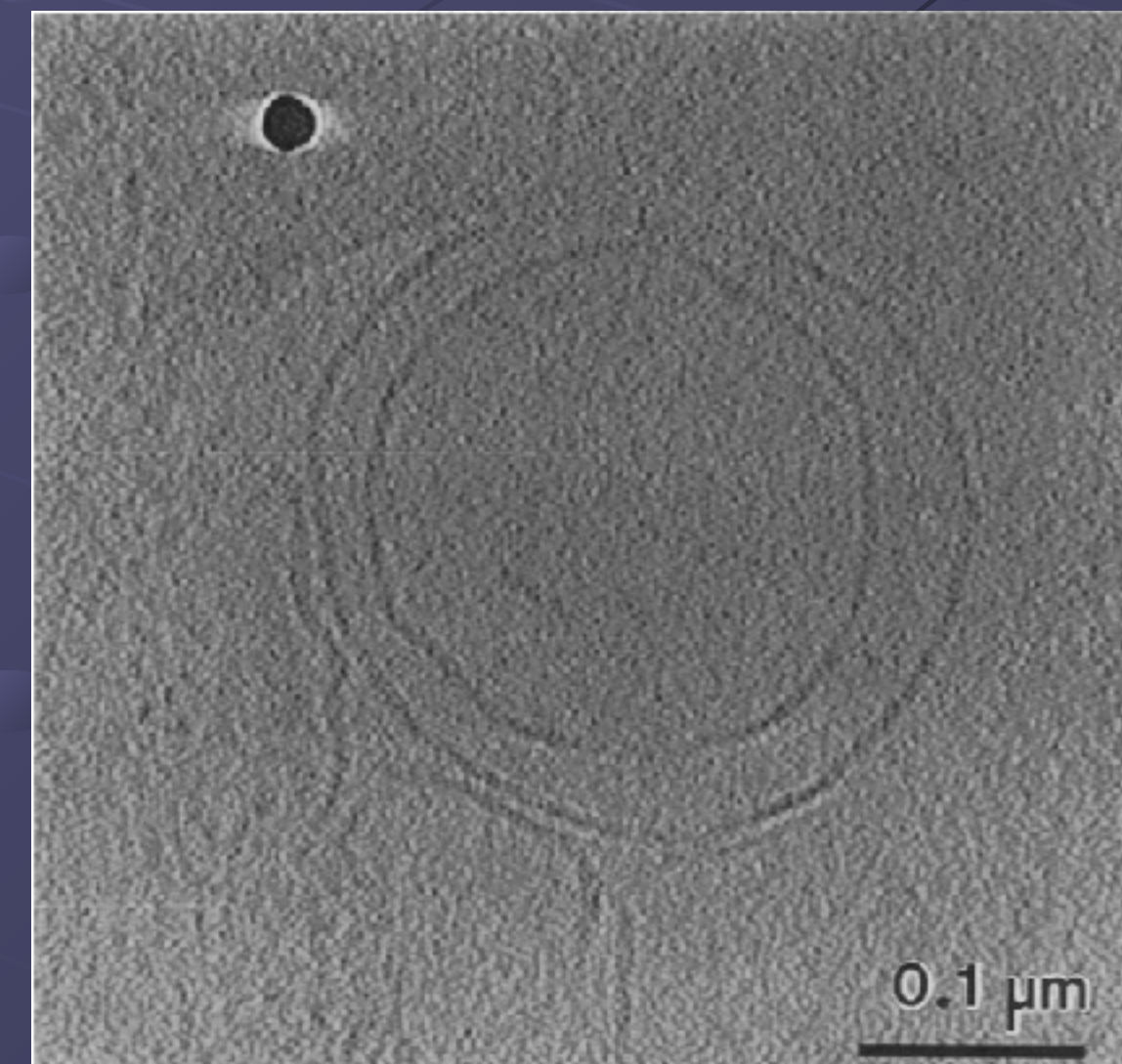


FIGURE 4 Central x-y section through the 3D reconstructed volume at full resolution, with frequency cutoff at $(5 \text{ nm})^{-1}$.

Tomography is possible with frozen hydrated samples!

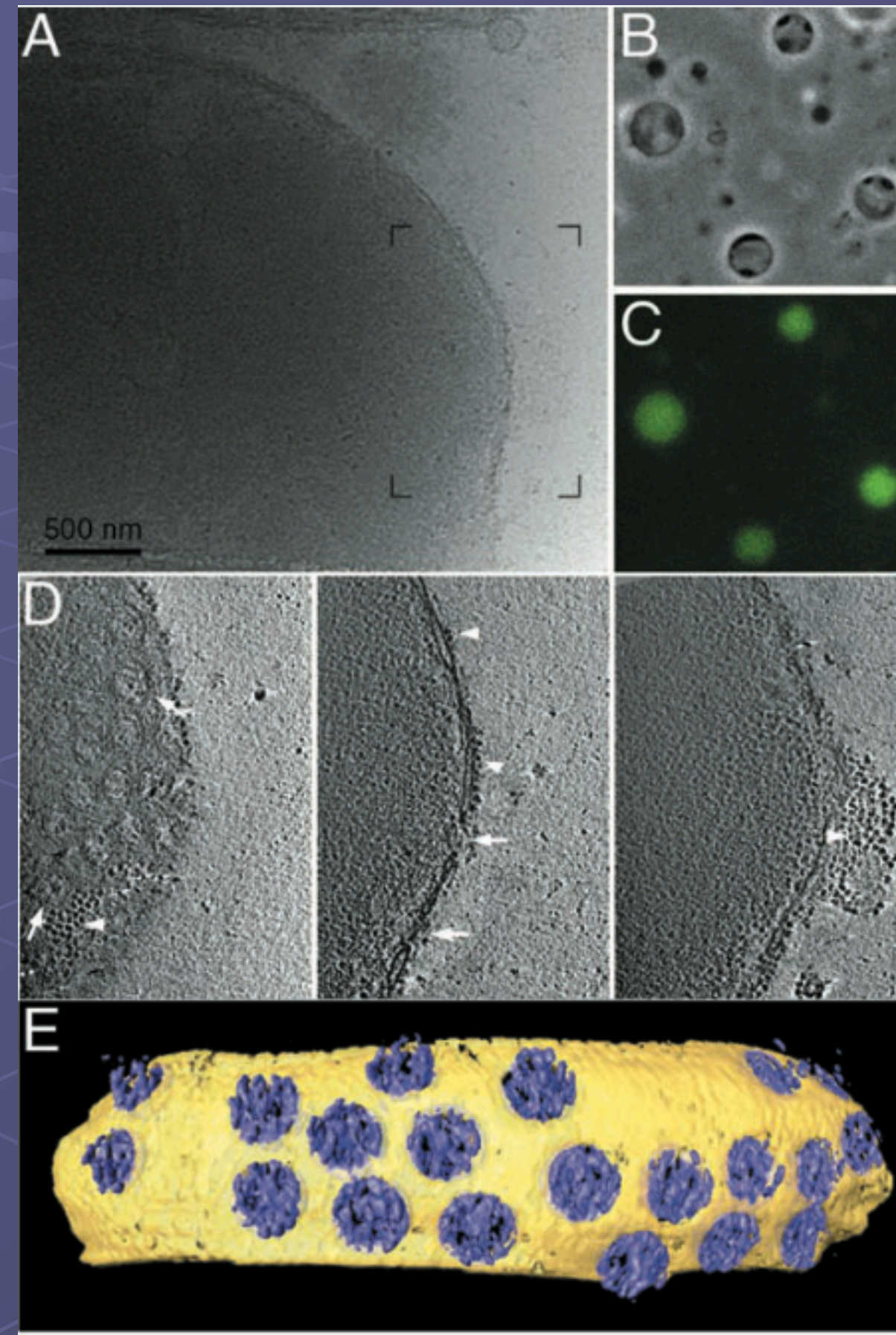
Sub tomogram averaging



Martin Beck



Juergen Plitzko



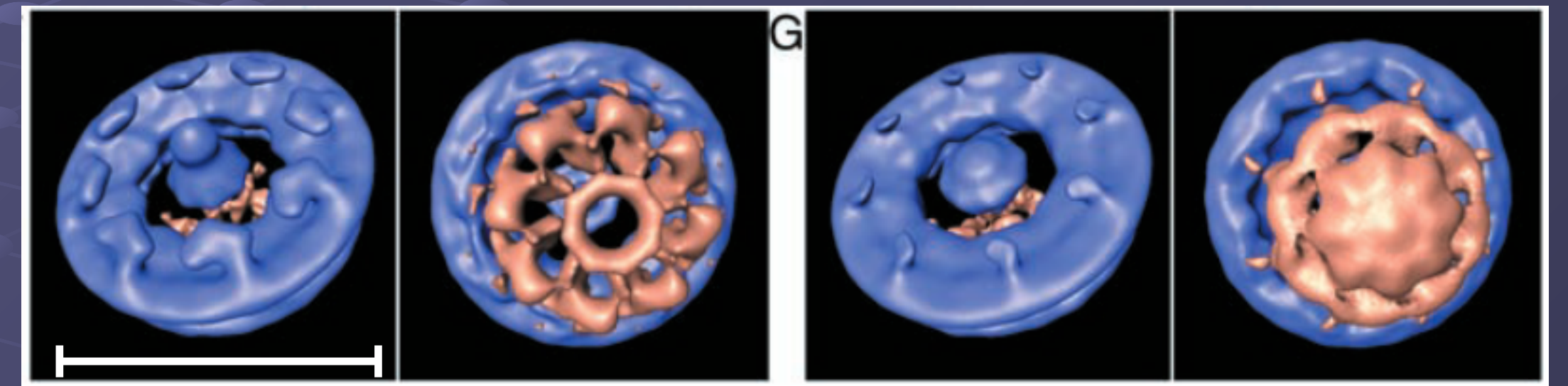
Cryo ET of 2 μ intact nucleus

Resolution ~9 nm

Sub tomogram averages

CF class

LR class

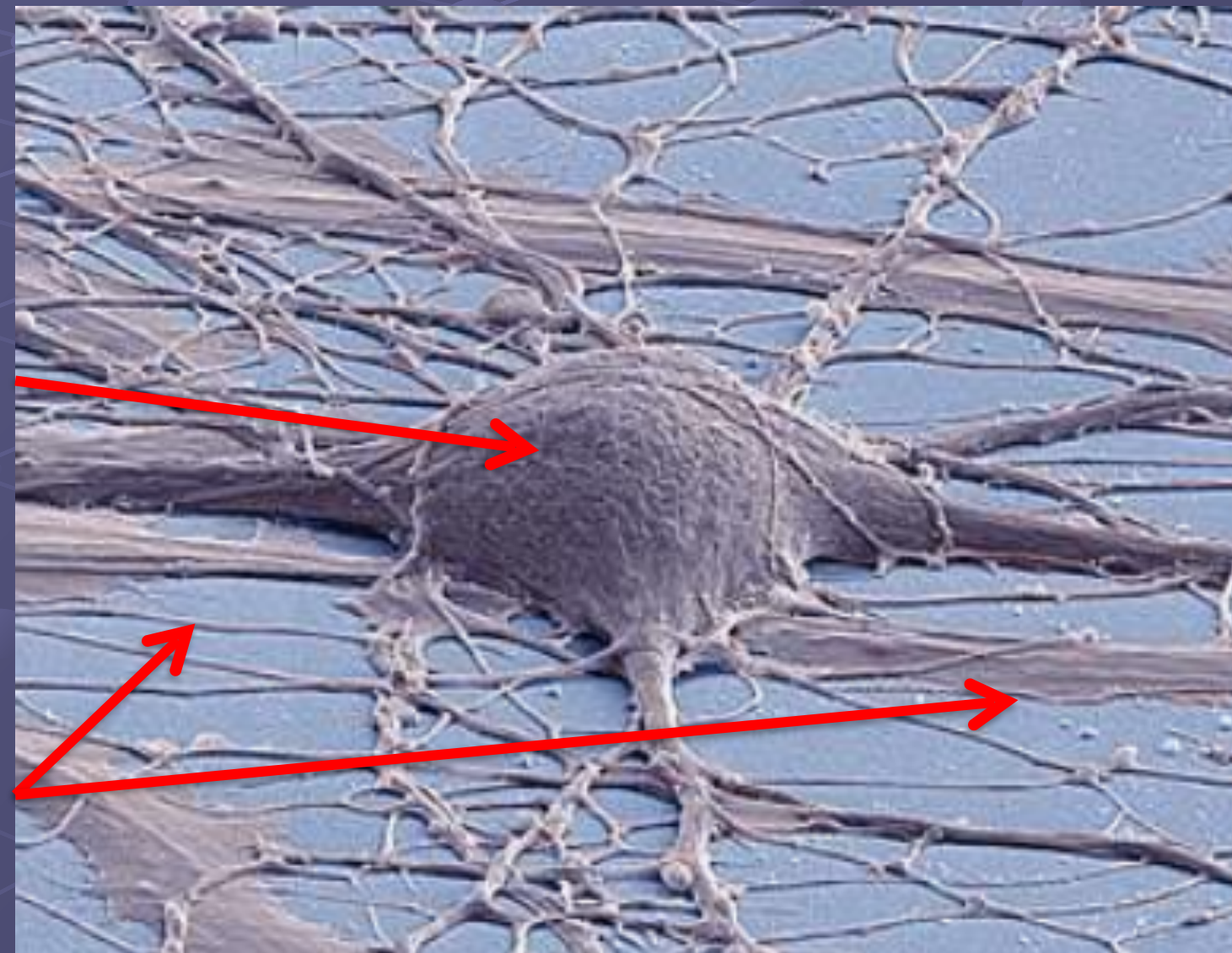


Sub tomogram averaging best resolution ~3Å!

Beck M, Förster F, Ecke M, Plitzko JM, Melchior F, Gerisch G, Baumeister W, Medalia O. Nuclear pore complex structure and dynamics revealed by cryoelectron tomography. Science. 2004 Nov 19;306(5700):1387-90.

The cell body is too thick to freeze well and too thick to get a beam through.

These are small enough to freeze well and to get the electron beam through.



This is a scanning electron micrograph (false color) of a human induced pluripotent stem cell-derived neuron. Credit: Thomas Deerinck, UC San Diego

Focused Ion Beam milling of frozen-hydrated E. coli

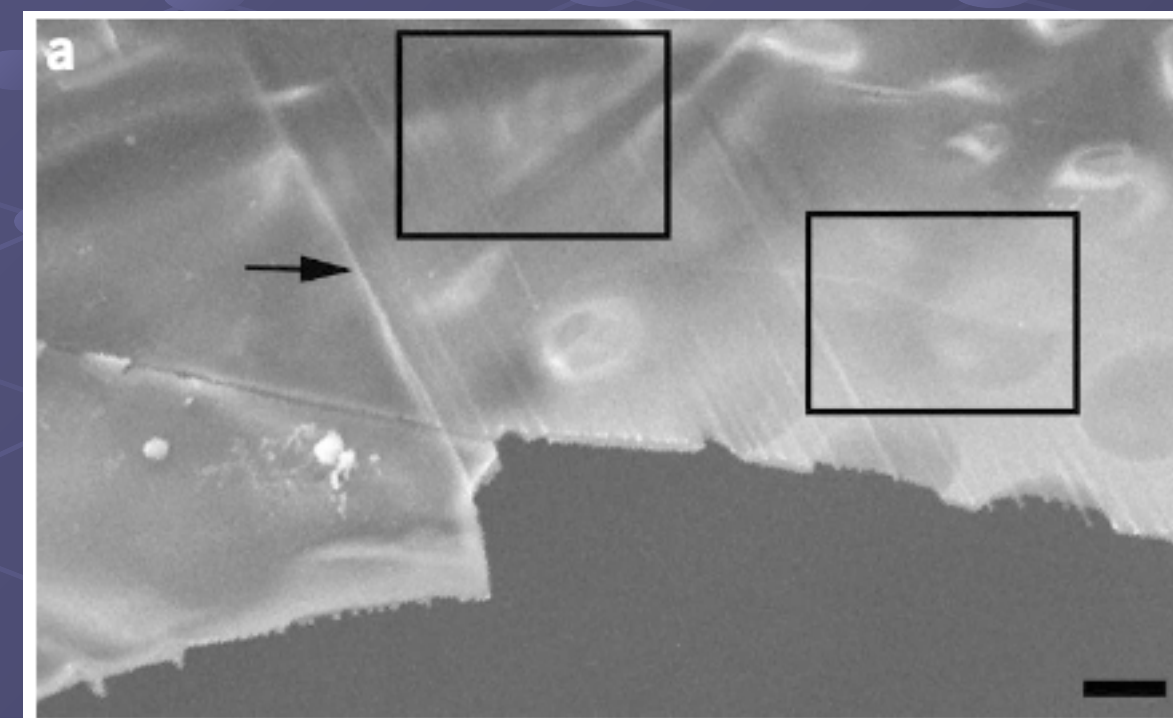
Tomogram with segmentation



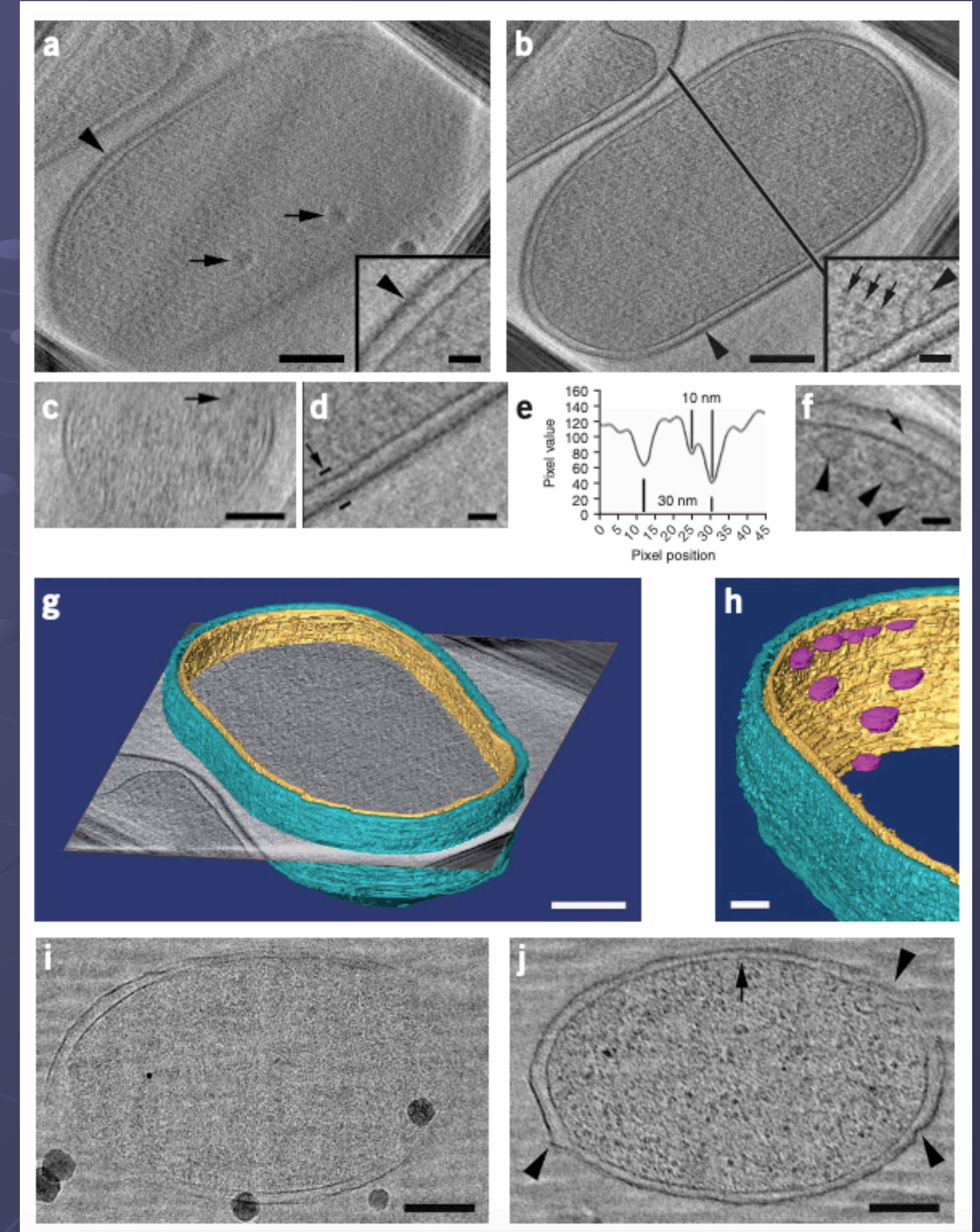
Mike Marko and Mui

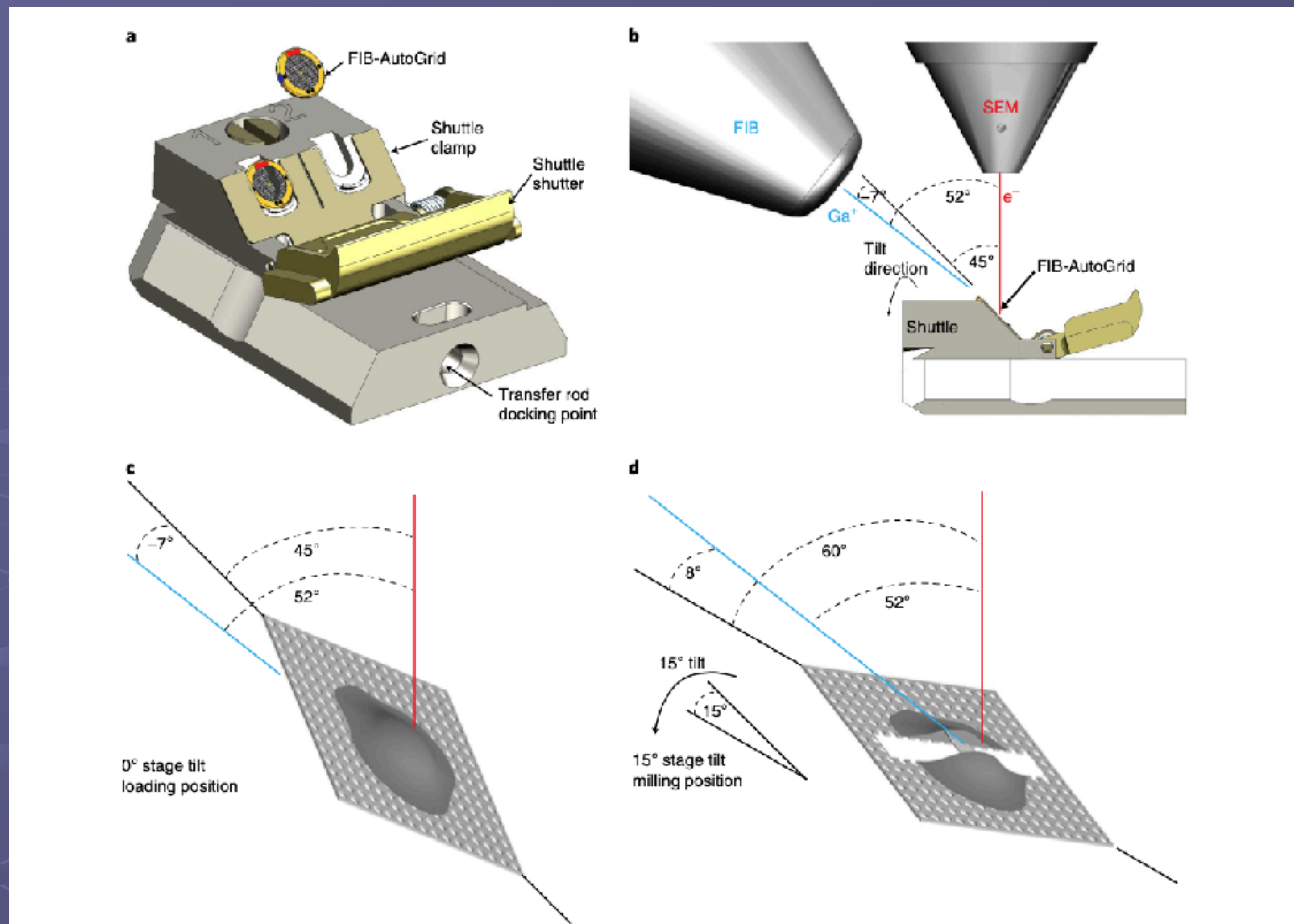
Varano, C. (2021). Mike Marko: Preserving the Past and Shaping the Future. *Microscopy Today*, 29(1), 56-57. doi:10.1017/S1551929520001741

Lamella



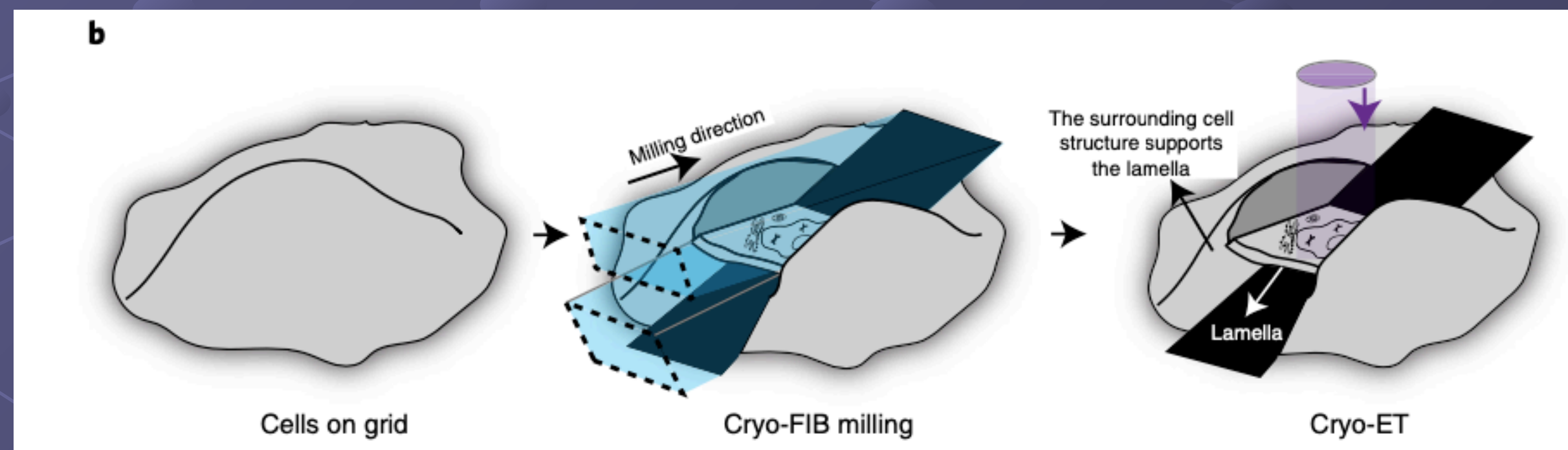
About 500 nm thick



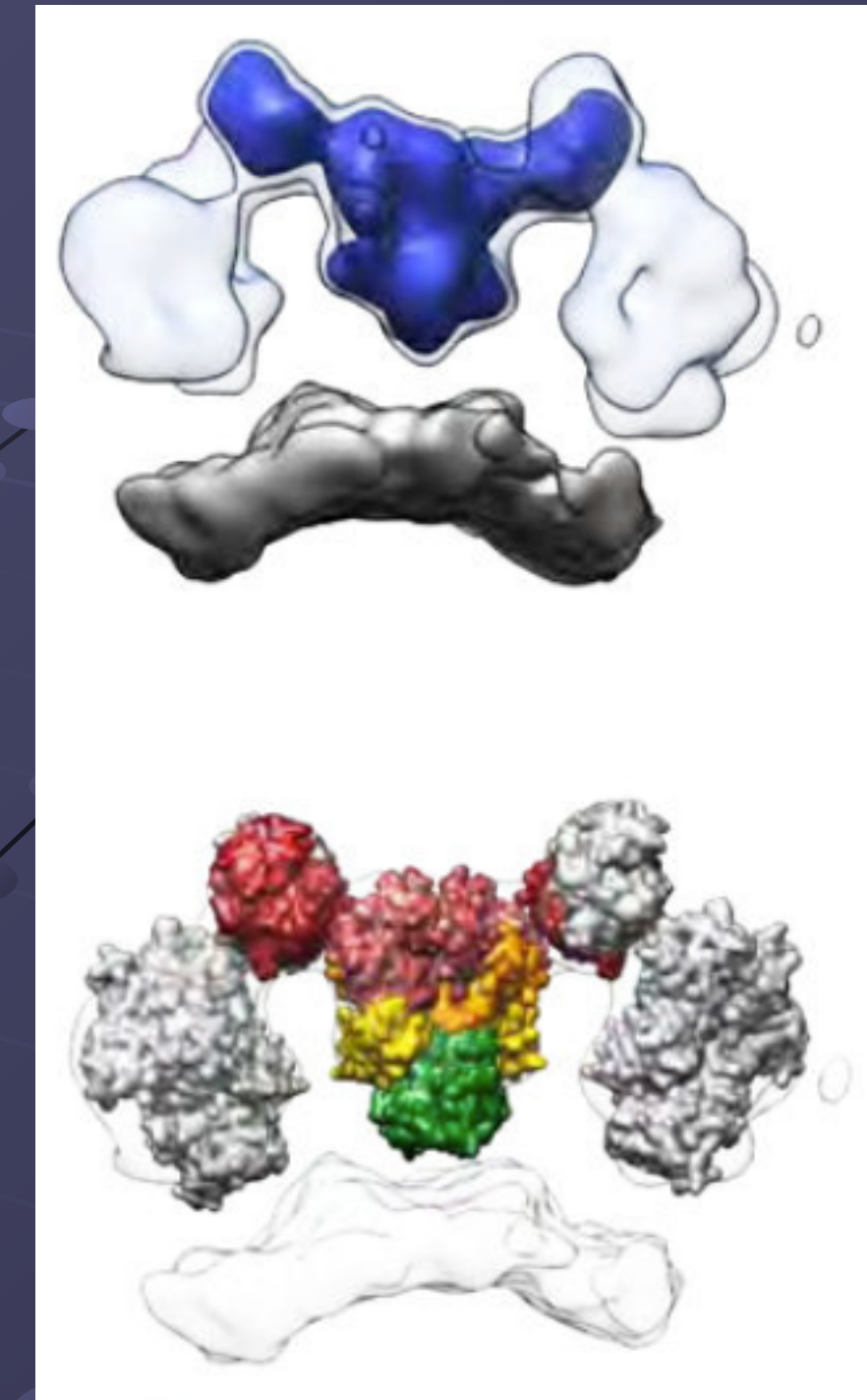
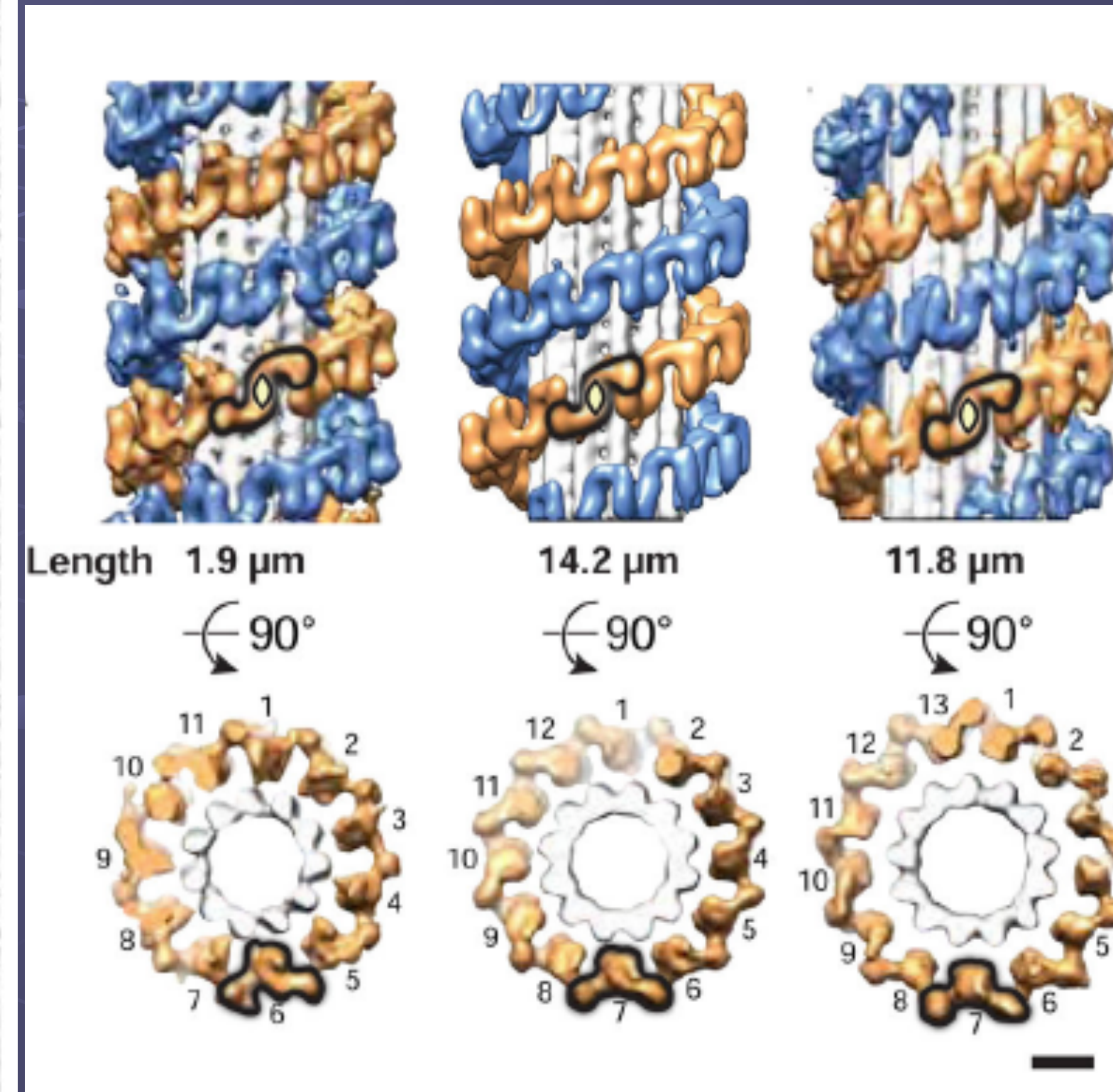
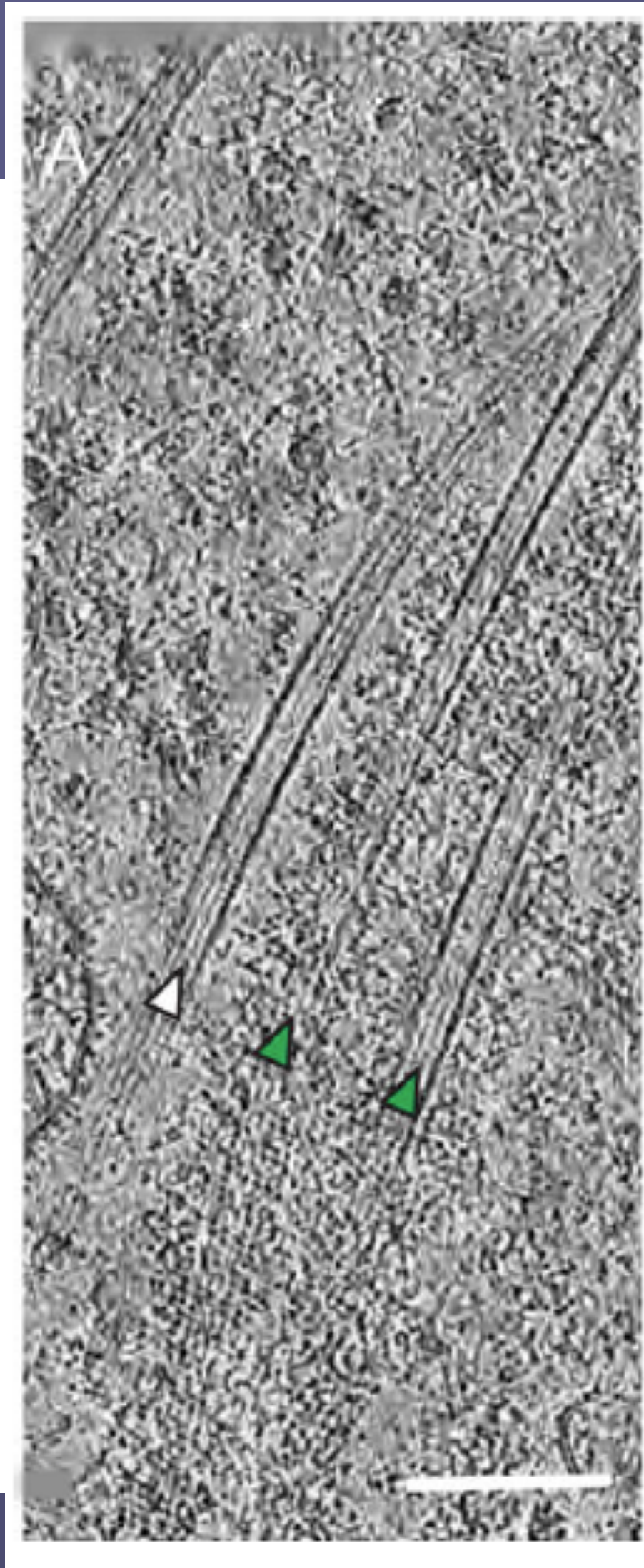
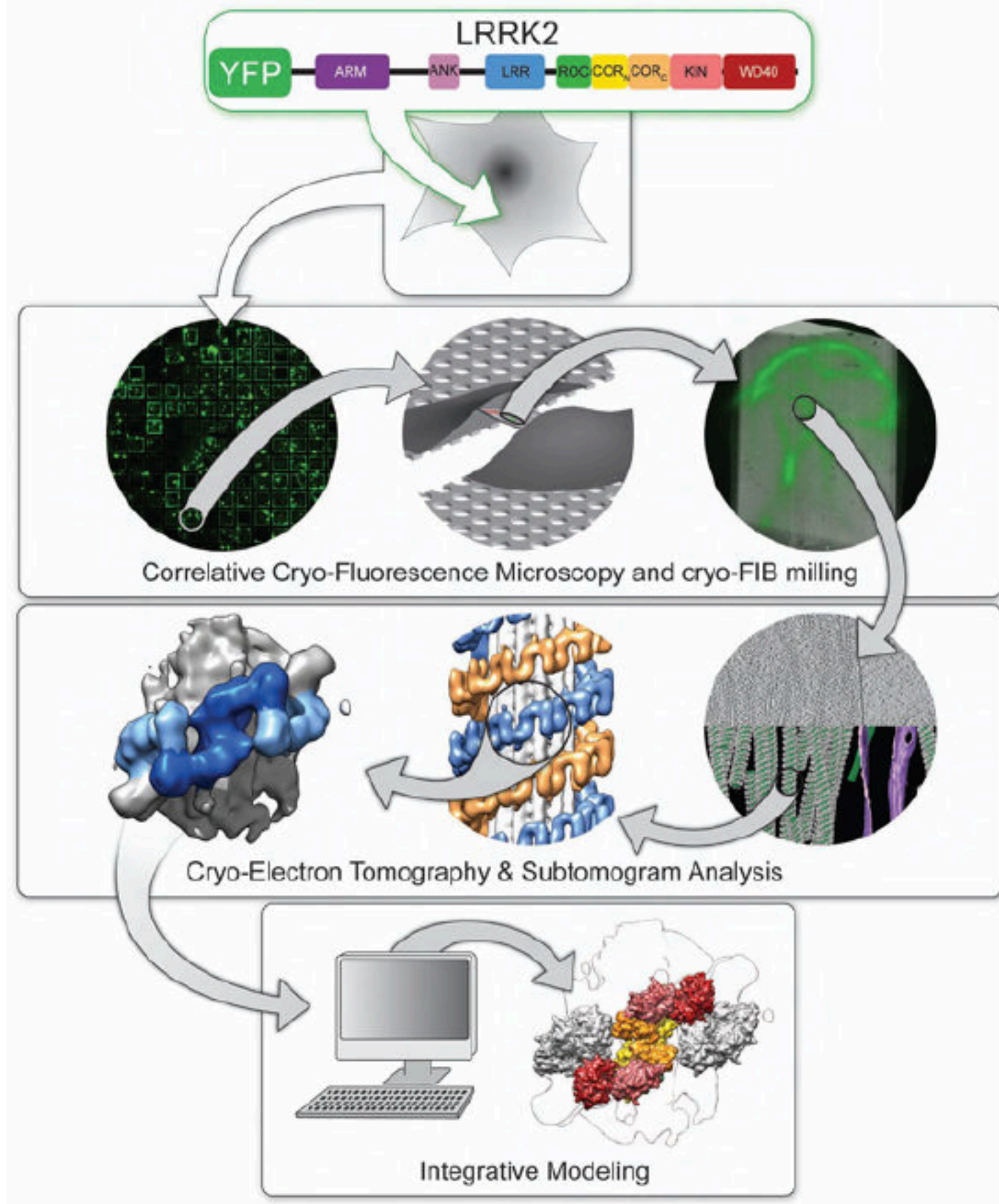


FIB-SEM as practiced today

Thick specimens can be sliced and subjected to cryo electron topography!



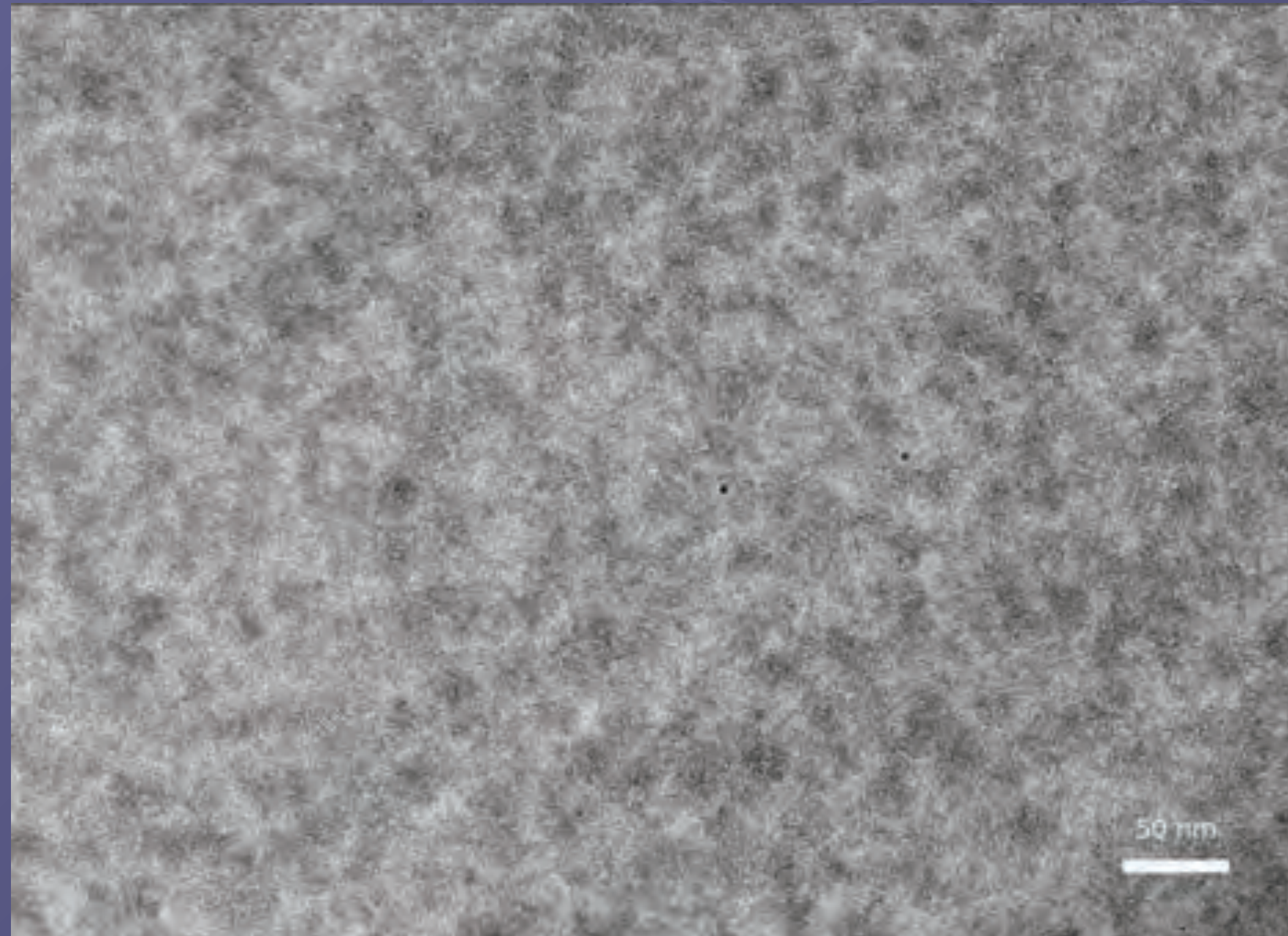
These two works are a perfect example of using FIB milling, cryo-ET, and subtomogram averaging.



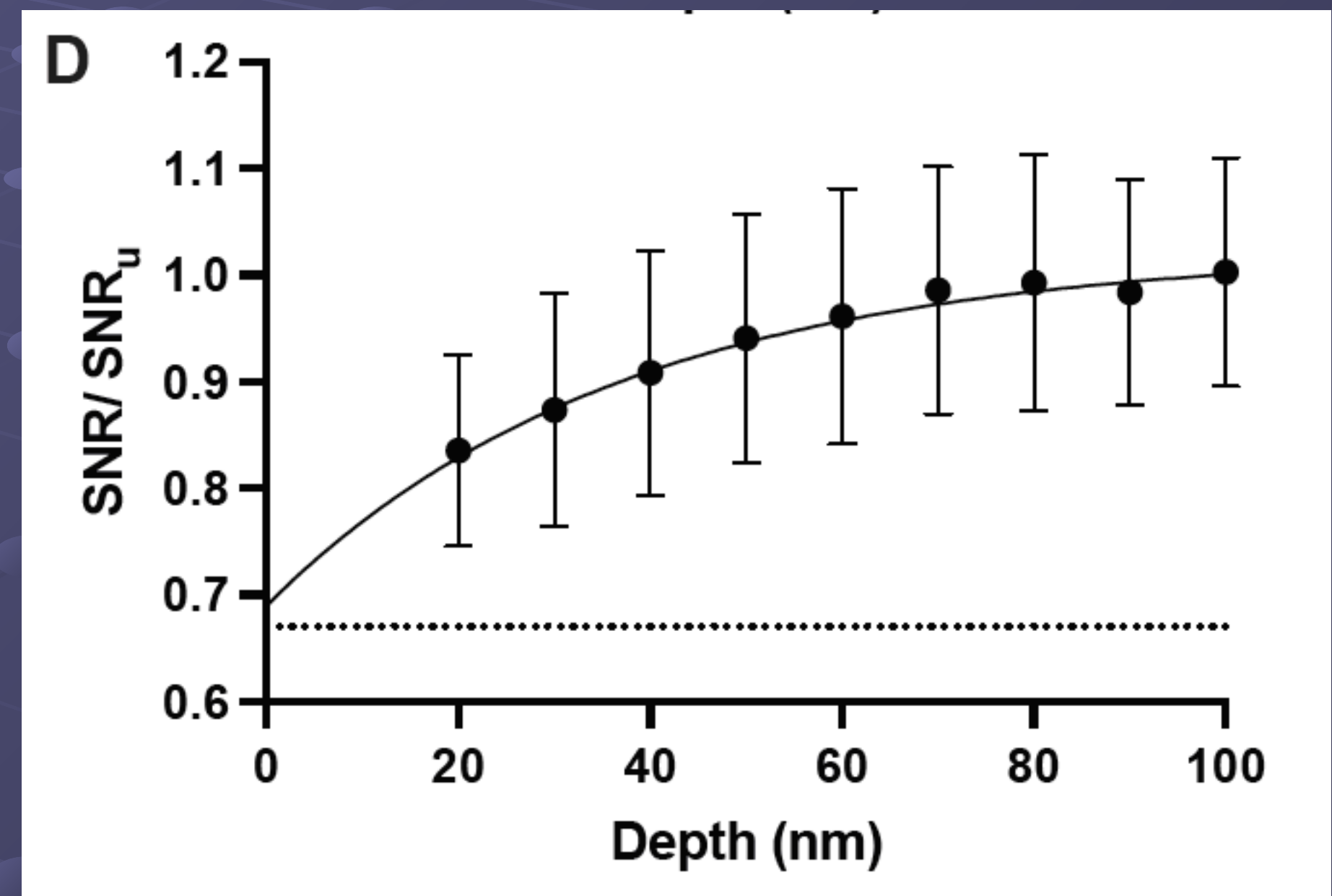
Watanabe R, Buschauer R, Böhning J, Audagnotto M, Lasker K, Lu TW, Boassa D, Taylor S, Villa E. The In Situ Structure of Parkinson's Disease-Linked LRRK2. *Cell*. 2020;182:1508-1518.

Deniston CK, Salogiannis J, Mathea S, Snead DM, Lahiri I, Matyszewski M, Donosa O, Watanabe R, Böhning J, Shiau AK, Knapp S, Villa E, Reck-Peterson SL, Leschziner AE. Structure of LRRK2 in Parkinson's disease and model for microtubule interaction. *Nature*. 2020;588:344-349.


FIB damages particles near the faces of the lamella



Lamella from yeast packed with ribosomes



The rise of SNR with distance from the lamella face



The
evolution,
deficiencies,
&
promise
of
cryo-electron microscopy

Images are not perfect projections of the desired 3D structure because:

Electrons damage the specimen.

Underfocus affects amplitudes and phases.

Digitization and boxing of the image affects and limits amplitudes and phases.

Coherence of the electron beam limits resolution.

Beam induced motion limits resolution.

Image distortion by the lenses affects phases.

Interpolation reduces high resolution amplitudes.

Beam tilt alters phases.

Lack of plane parallel illumination alters phases.

Insufficient depth of field alters amplitudes and phases.

Multiple scattering alters amplitudes and phases.

Not all scattered electrons are imaged.

Tomograms are not perfect 3D maps of structure because (in addition to the items in the previous page):

The tilt angle is limited to ~60 degrees (known as the missing wedge).

The incremental step in angle is limited by dose.

The milling beam damages the outer layers of a lamella.

We are limited to a small volume of the cell (serial sectioning is not possible).

The entire process of milling and imaging is slow.

We can fail to include our structure of interest when we mill a lamella.

Lamellae can break or twist.

We can get ice contamination on our lamella.



The
evolution,
deficiencies,
&
promise
of
cryo-electron microscopy

What we can expect or hope for in single particle cryo-EM to get us all to $<2\text{\AA}$:

A stable phase plate will allow us to determine structures of $mw = 12,500$ (Henderson limit).

Update: The laser phase plate provides almost perfect, stable phase contrast.

A simple reliable method for loading samples onto grids with thin ice, no denaturation at the air water interface, and avoids preferred orientation.

Complete automation from grid preparation to atomic model.

Easy access from images to the energy landscape of conformational forms; we want to visualize images and distributions of conformations within our structures.

What we can expect or hope for in cryo ET: complete segmentation of all structures in a tomogram.

Better lamella production: limited damage from FIB-SEM, no ice contamination, and no broken lamellae.

Localization of fluorescent markers with an error $<\sim 10\text{nm}$ and transfer of coordinates to the FIB-SEM for milling and to the lamella for eventual segmentation.

Structural tags as opposed to fluorescent tags for structures of interest.

Identification and location of structures of interest with a tomogram.

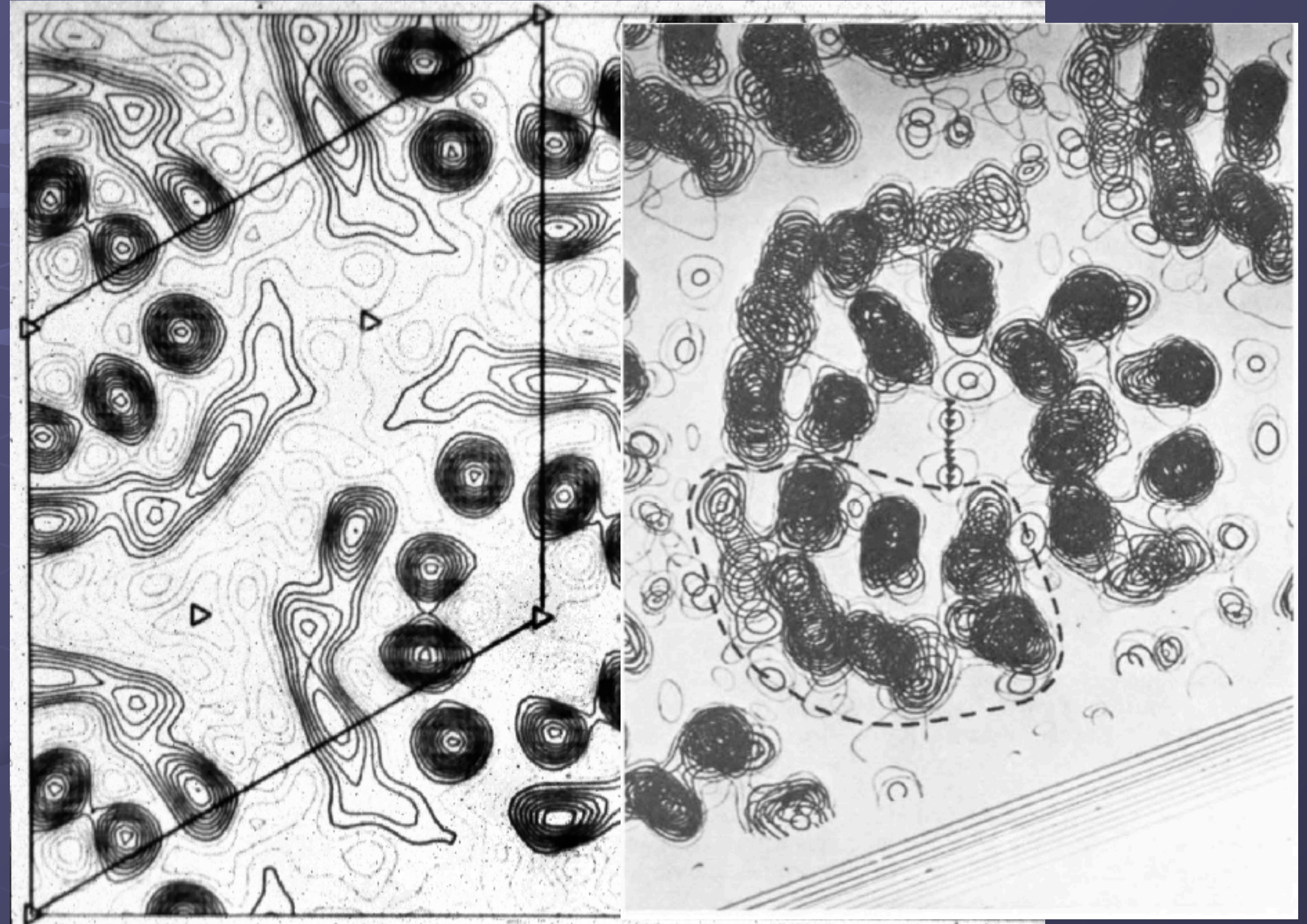
We over estimate what will be done in the short term and under estimates what will be done in the long term.
(Bob Glaeser quotes this - the originator of the expression is unclear).

This was the first time we could see the protein itself instead of the hole it left in the negative stain, and it was the first view of a membrane protein albeit in projection.



Nigel Unwin and Richard Henderson

Glucose was not a good embedding agent for single particles because the particles were 'hidden' by the glucose.



Averaged (projection) image of bR

Resolution = 7 Å

